ACS OMEGA

Open Access

http://pubs.acs.org/journal/acsodf

Article

3-Acetyl-11-keto-β-boswellic Acid-Based Hybrids Alleviate Acetaminophen-Induced Hepatotoxicity in HepG2 by the Regulation of Inflammatory and Oxidative Stress Pathways: An Integrated Approach

Abdullah A. Elgazar, Ramadan A. El-Domany, Wagdy M. Eldehna, and Farid A. Badria*

Cite This: *ACS Omega* 2023, 8, 39490−39510

Read Online

ACCESS | Metrics & More | Article Recommendations | Supporting Information

ABSTRACT: In an effort to develop new compounds for managing drug-induced liver injury, we prepared 23 novel hybrids based on 3-acetyl-11-keto-β-boswellic acid (AKBA) using various biocompatible linkers. A bioguided approach was employed to identify the most promising hybrid. Eight compounds exhibited superior anti-inflammatory activity compared to the parent compound. Two of these hybrids (**5b** and **18**) were able to reduce gene expression of TNF-α in LPS-induced inflammation in RAW 264.7 cells, similar to dexamethasone. Subsequently, the hepatoprotective potential of these hybrids was evaluated against acetaminophen (APAP) toxicity in HepG2 cells at doses of 1 and 10 μM. Both hybrids effectively restored cytokine levels, which had been elevated by APAP, to normal levels. Furthermore, they normalized depleted superoxide dismutase and reduced glutathione levels while significantly reducing malondialdehyde (MDA) levels. Network pharmacology analysis suggested that AKBA-based hybrids exert their action by regulating PI3K and EGFR pathways, activating anti-inflammatory mechanisms, and initiating tissue repair and regeneration. Molecular docking studies provided insights into the interaction of the hybrids with PI3K. Additionally, the hybrids demonstrated good stability at different pH levels, following first-order kinetics, with relatively long half-lives, suggesting potential for absorption into circulation without significant degradation.

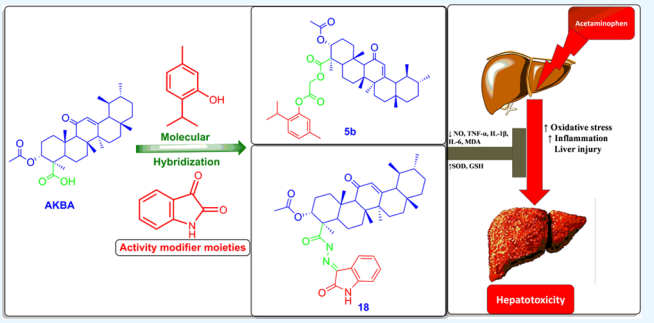

1. INTRODUCTION

The recent advances in molecular biology changed our perspective on the management of chronic ailments. It is now realized that monotherapy for such diseases has several drawbacks on both therapeutic and pharmacoeconomic levels. This means that more holistic approaches are required to achieve sustainable health outcomes and decrease the associated economic burden.[1]

Instead, polypharmacological approaches would be the best alternative. This could be accomplished by developing pharmacological agents that could target several pathways responsible for disease development. Here comes the revisiting of natural products (NPs) as promising bioactive compounds with multiple therapeutic activities to manage complex health disorders, and there are continuous quests to maximize the available wealth of structure−property information on natural products and characteristic salient molecular features of NPs.[2−4]

Not surprisingly, the development of bioactive hybrid form NPs has been an active area for research. Specifically, triterpenes, which are natural compounds widely abundant in plants, have been subjected to extensive research to improve both their pharmacodynamics and pharmacokinetics through conjugation with other bioactive synthetic or natural substrates. For instance, oleanolic acid was conjugated with azidothymidine, leading to an antiviral hybrid;[5] also, conjugation of boswellic acid with Rhein as a mutual prodrug led to significant enhancement in the absorbance of the parent drugs and more pronounced anti-inflammatory activity.[6]

This was also the case when boswellic acid was conjugated with ibuprofen to obtain a hybrid with dual COX-2 and 5-LOX inhibitors that did not cause an ulcerogenic effect *in vivo*.[7] The conjugation of a chalcone scaffold with AKBA also leads to improved cytotoxic activity due to its ability to inhibit pin-1 at (IC_{50} = 0.97 μM) to AKBA (IC_{50} = 50 μM).[8] In another study, click chemistry was used for the formation of boswellic acid triazole hybrids, which give potent α-glucosidase inhibitory

Received: July 20, 2023
Accepted: September 28, 2023
Published: October 12, 2023

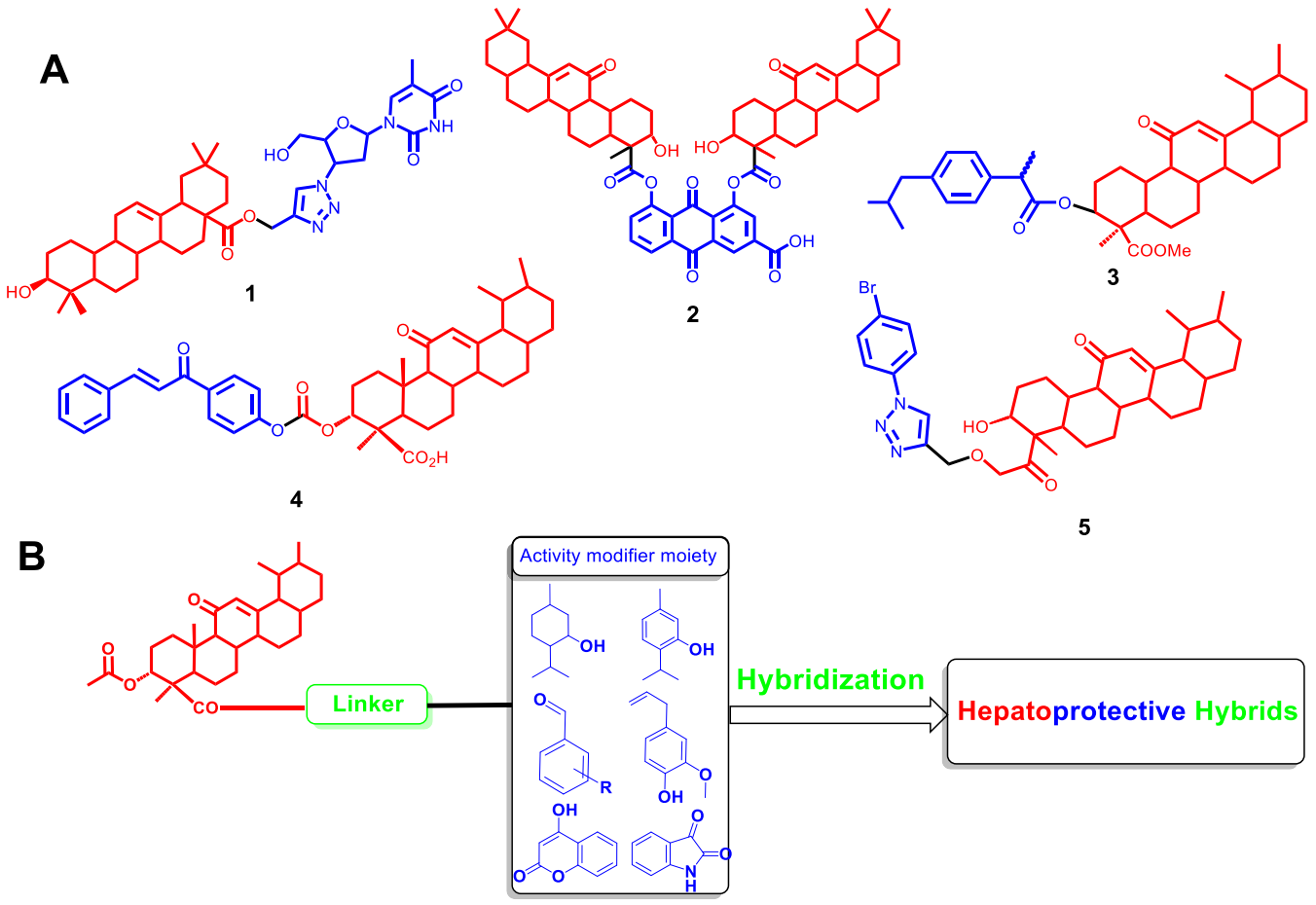

Figure 1. (A) Some examples of hybrids based on triterpenes: (1) oleanolic acid−azidothymidine hybrid, (2) boswellic acid−Rhein, (3) boswellic acid−ibuprofen hybrid, (4) AKBA−chalcone hybrid, and (5) AKBA−triazole hybrid. (B) Strategy for modifying the activity of acetyl keto boswellic acid to produce hepatoprotective hybrids by conjugation with natural moieties with reported antioxidant activity.

Scheme 1. Steglich Esterification of AKBA with Menthol or Thymol to Obtain Esters 3a-b

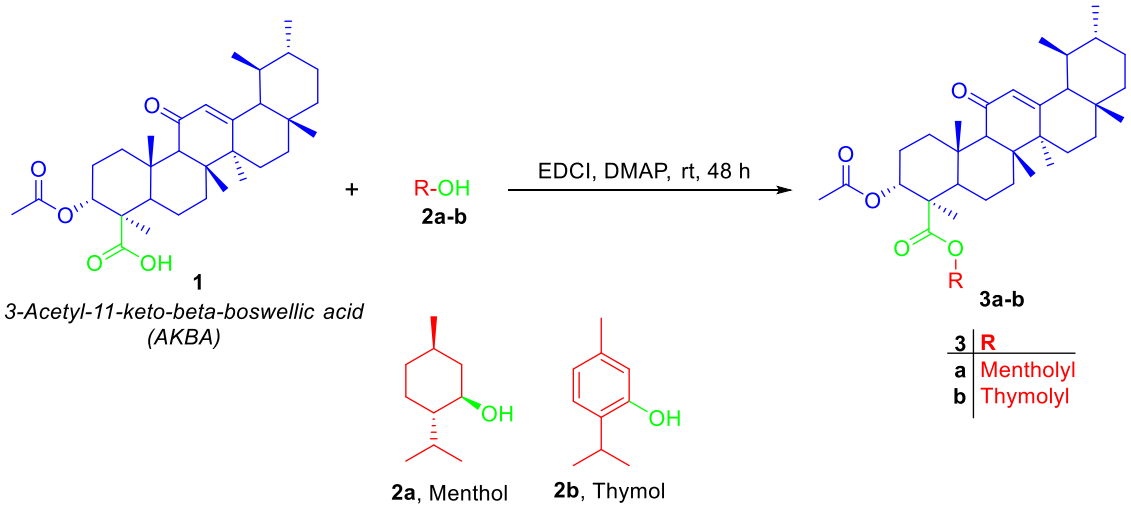

activity (IC_{50} = 0.43 μM) in comparison to standard acarbose (IC_{50} = 942 μM),[9] as shown in Figure 1A.

In this context, oleogum resin from frankincense was reported to possess hepatoprotective properties;[10−12] among its constituents, boswellic acids are extensively studied, especially 3-acetyl-11-keto-β-boswellic acid (AKBA), which emerged as a potent anti-inflammatory agents[13−15] Moreover, AKBA is known to bind to receptors in bile and help in restoration of liver normal architecture.[16] So, hybrid pharmacological agents could serve as a promising solution to multifaced conditions[17] such as drug-induced hepatitis, which affects the lifestyle of thousands of patients and may develop into life-threatening situations.

https://doi.org/10.1021/acsomega.3c05247
ACS Omega 2023, 8, 39490−39510

Scheme 2. Preparation of Acetylated Derivatives 5a−d through the Conjugation of Bromoacetyl Bromide with Respective Phenols or Alcohols, Which Then Was Reacted with AKBA

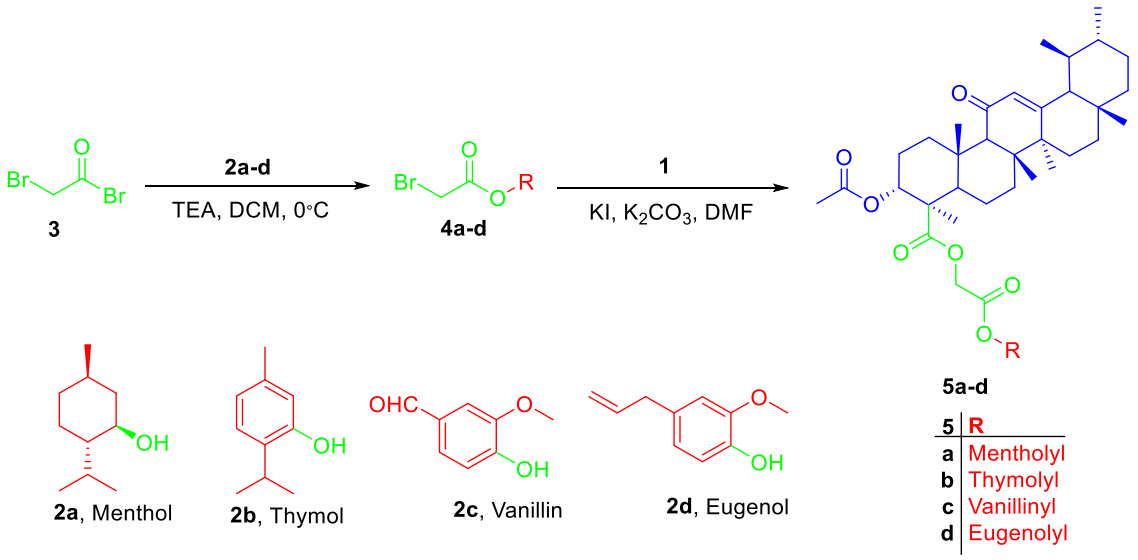

Scheme 3. Preparation of AKBA Hybrids 8a−c

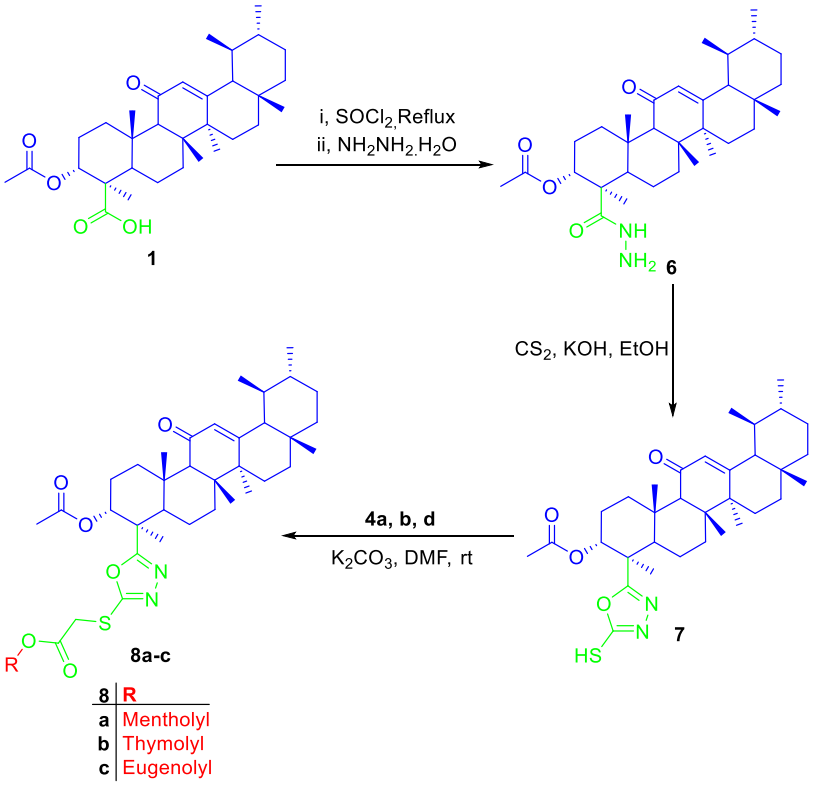

Acetaminophen (APAP), one of the most used analgesic and antipyretic agents, is known to cause liver injury in the case of overdose due to its notorious metabolite *N*-acetyl-*p*-benzoquinone imine (NAPQI), which could lead to permanent liver failure if not managed rapidly. The antioxidant N-acetyl cysteine has been prescribed concomitantly with APAP to avoid such serious effects. However, the complexity of NAPQI-induced toxicity requires the regulation of several pathways related to inflammation, oxidative stress, and tissue regeneration.[18,19] So, conjugation of AKBA with other antioxidant and hepatoprotective moieties could be a promising approach for the prevention and management of drug-induced liver injury (Figure 1B)

In our lab, we attempted new approaches to explore and modify bioactive natural products using molecular biology tools, *in silico* investigations, derivatization strategies, and pharmaceutical formulations.[20−27] So, the successful stories of hybridization of boswellic acids as anti-inflammatory, cytotoxic agents, and antidiabetic agents[28−30] encouraged us to pursue novel new hybrids based on AKBA and other anti-inflammatory and antioxidant natural products; these hybrids will be evaluated for their ability to mitigate APAP toxicity *in*

https://doi.org/10.1021/acsomega.3c05247
ACS Omega 2023, 8, 39490−39510

Scheme 4. Preparation of AKBA Triazole Hybrids 14a−c

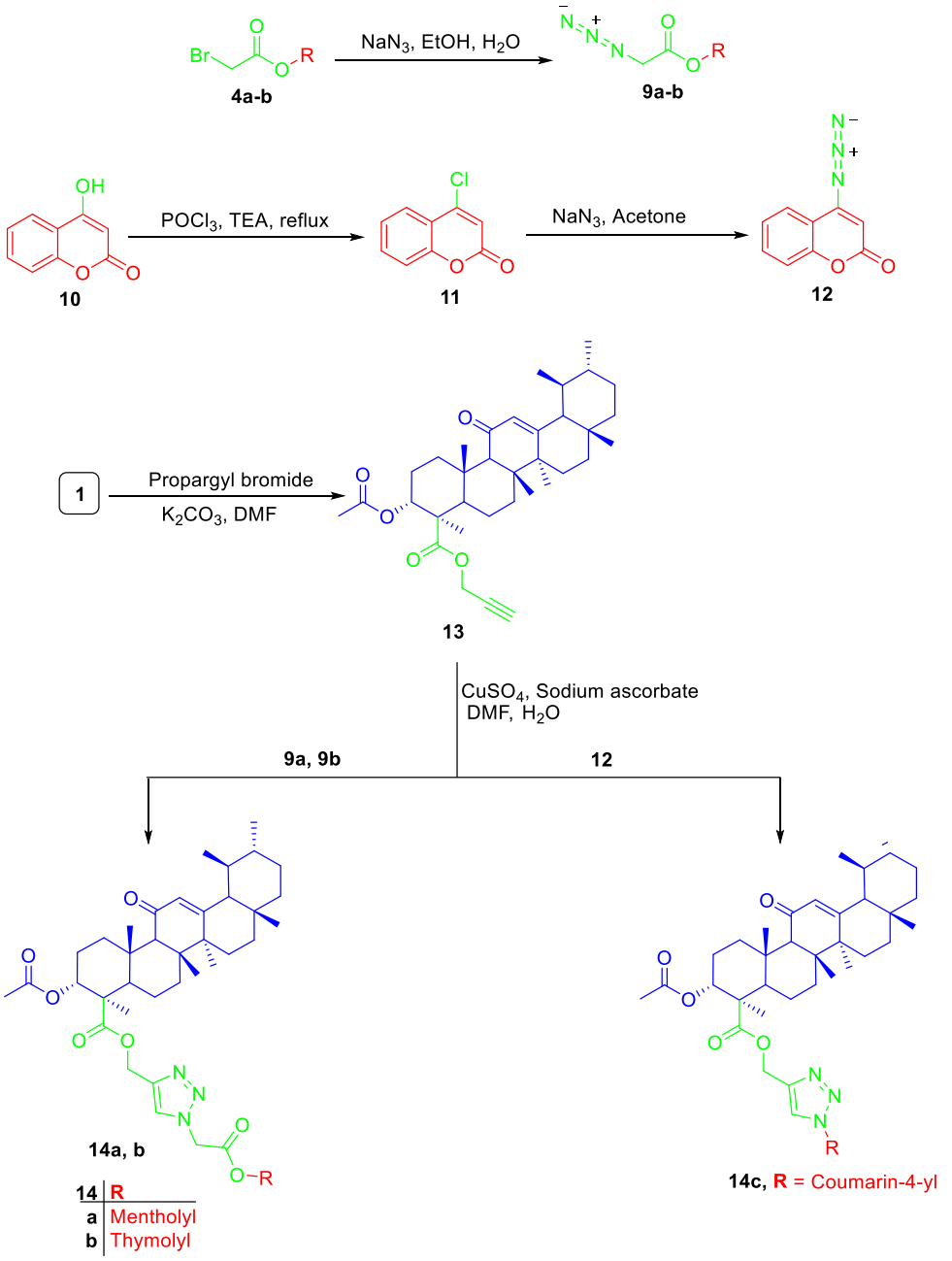

vitro. Furthermore, gene enrichment for the elucidation of potential targets of the compounds would be addressed and supported by molecular docking studies. Finally, their stability in a simulated gastric and intestinal environment would be assessed.

2. RESULTS AND DISCUSSION

2.1. Chemistry. In this work, we aimed at the preparation of AKBA hybrids and assessed their therapeutic activity and pharmacokinetic properties. AKBA hybrids were obtained through Steglich esterification by a reaction with natural compounds, such as menthol, 4-hydroxy coumarin, thymol, eugenol, and vanillin, in the presence of EDCI as a coupling agent,[31] as shown in Scheme 1, or bromoacetyl bromide derivatives, as shown in Scheme 2, while the formation of 1,2,3-triazole-based hybrids was possible by reacting the propargyl derivative of AKBA with respective azides, as shown in Scheme 3. Finally, the synthesis of 1,3,4-oxadiazole and hydrazone hybrids was achieved by reacting the hydrazide derivative with carbon disulfide, which was alkylated with bromoacetyl derivatives, or by reacting it with aromatic aldehydes and isatin, as illustrated in Schemes 4 and 5, respectively. The relatively low yield was attributed to the use of normal-phase silica in the purification, whereas much better yields could be obtained when reversed-phase column chromatography was used

The prepared hybrids showed a characteristic spectroscopic profile, which is commonly found in ursane-type triterpene. For instance, ^{13}C NMR spectra showed three peaks at 198, 165, and 13 ppm, corresponding to C-11, C-12, and C-13, respectively, and two esters functional at 170 and 175 ppm, which were assigned to C-24 and C-3, respectively. Meanwhile,

https://doi.org/10.1021/acsomega.3c05247
ACS Omega 2023, 8, 39490−39510

Scheme 5. Preparation of AKBA Hydrazone Hybrids by Reacting Acid Hydrazide with Different Aldehydes or Ketones

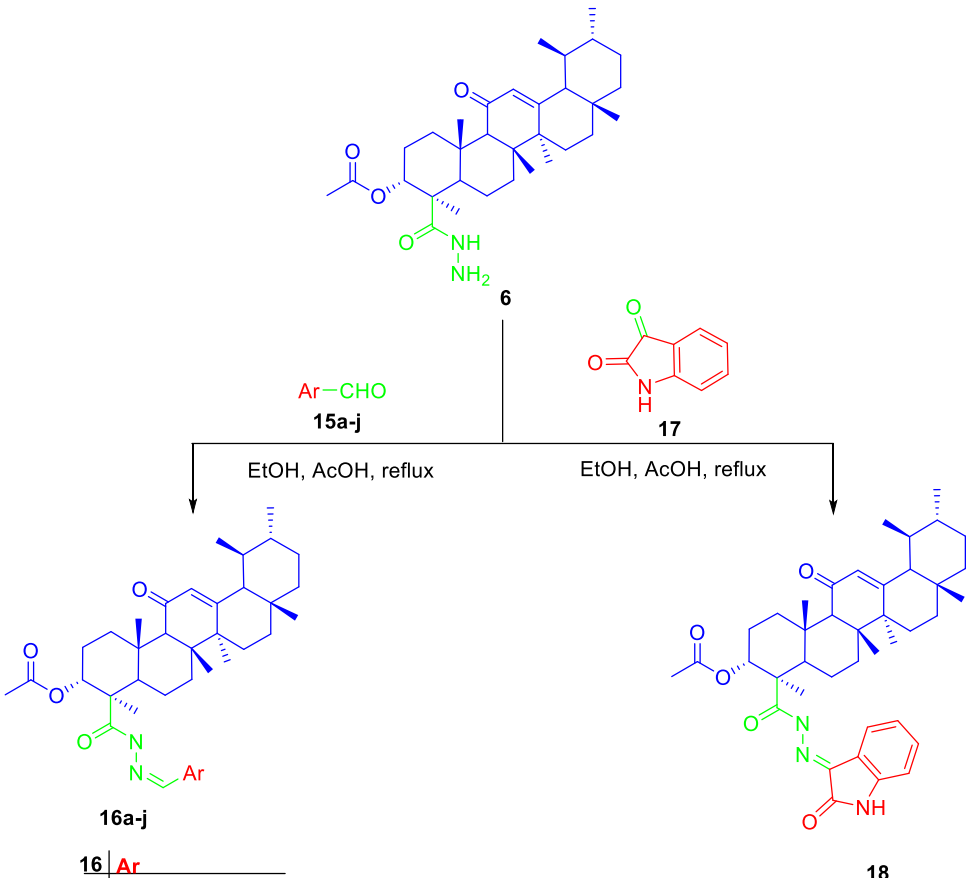

16	Ar
a	C_6H_5
b	2,5-$OCH_3C_6H_3$
c	3,4-$OCH_3C_6H_3$
d	3,4,5-$OCH_3C_6H_2$
e	3-$OCH_3C_6H_4$
f	2-OHC_6H_4
g	3,4-OCH_2O-C_6H_3
h	3-OH,4-$OCH_3C_6H_3$
i	4-$OCH_3C_6H_4$
j	-CH=CH-Ph

^{1}H NMR spectra showed a singlet proton at 5.4 ppm assigned for an olefinic proton at C-12, which is representative of an $\alpha-\beta$ unsaturated ketone moiety. Moreover, the presence of oxy-carbon at position 3 was confirmed by proton at 5.2 ppm in ^{1}H NMR and 72.2 ppm in ^{13}C NMR. Other protons of the triterpene skeleton were observed at around 2.6−0.6, as previously reported in the literature.[32]

For hybrids prepared through Steglich esterification, the spectroscopic data exhibited the same pattern in line with the previously reported data for the starting compounds except for the observed reduction of the chemical shift value from 180 to 168 ppm, confirming the transformation of the acid group of AKBA to ester. Regarding the menthol hybrid, an increase in the chemical shift value of proton 1′ of menthol from 3.4 to 4.6 ppm was found, while in the case of the thymol hybrid, aromatic protons shifted from 7.3 to 7.5 ppm, as shown in Tables S1 and S2. Eugenol and vanillin derivatives were unstable and hydrolyzed rapidly

On the other hand, AKBA hybrids were prepared with an acetyl spacer via reacting AKBA with a bromoacetyl derivative of the corresponding alcohol or phenol. The produced AKBA hybrids using an acetyl spacer showed an additional peak at around 4.6 ppm (s, 2H) in ^{1}H NMR and 61 and 166 ppm in ^{13}C NMR, indicating the presence of the acetyl linker, as presented in Tables S3−S6.

Additionally, hybrids **8a−c** containing 1,3,4-oxadiazole were prepared by reacting acid **1** with thionyl chloride to form the intermediates that possess a better-leaving group, acid chlorides, which further reacted with hydrazine hydrate to furnish hydrazide **6**. The latter reacted with carbon disulfide in a basic medium to form the oxadiazole linker, which was reacted with the bromoacetyl derivative of the corresponding alcohol or phenol. Therefore, these hybrids showed PMR behavior similar to previously discussed acetyl derivatives but showed a new peak at around 162 ppm in ^{13}C NMR, implying the presence of an oxadiazole ring; also, C-24 showed a decrease in the chemical shift from 180 to 167.4 ppm, as shown in Tables S7−S9. The vanillin-tethered derivative was not included as it was unstable and hydrolyzed rapidly before analysis and could not be isolated from the reaction mixture.

For yielding compounds containing a 1,2,3-triazole linker, bromoacetyl derivatives of menthol, thymol, or 4-chlorocou-

https://doi.org/10.1021/acsomega.3c05247
ACS Omega 2023, 8, 39490−39510

marin converted to the corresponding azide that reacted with the propargyl derivative of AKBA **13** through copper-catalyzed azide−alkyne cycloaddition, which was confirmed by the additional peaks at around δ 8.0 ppm (1H), corresponding to the triazole ring; also, three new peaks were observed in ^{13}C NMR assigned to the triazole carbons and the methylene between AKBA and the triazole ring at 142, 122, and 60 ppm, respectively, as shown in Tables S10−S12. It is worth noting that vanillin and eugenol derivatives were unstable and hydrolyzed rapidly during the reaction.

Nevertheless, no significant change was observed in the chemical shift values of the hybrids when compared to the parent compounds, as reported in the literature.[33] Still, atom carbon 4′ in 4-hydroxy coumarin-based hybrids showed a noticeable decrease in the chemical shift from 162 to 154 ppm, confirming the formation of the corresponding azide.

Finally, the hydrazone derivatives were prepared by the reaction of different aldehydes with AKBA hydrazide. This was confirmed by the appearance of two new signals (at 11 and 8 ppm) corresponding to the hydrazone linker protons and the disappearance of the proton at 9−10 ppm corresponding to the aldehyde protons; also, the decrease in the chemical shift of aldehyde carbon from 190 to 140 ppm indicates the formation of an AKBA−hydrazone hybrid. For an isatin hybrid, the hydrazone linker was observed at 11.36 and at 143.21 ppm, as shown in Tables S13−S23.

2.2. Biological Evaluation. *2.2.1. In Vitro Anti-inflammatory Assessment of AKBA Hybrids. 2.2.1.1. RAW 264.7 Cell Line Stimulated Inflammation by LPS.* Since AKBA is the main scaffold of the prepared hybrids, it was proposed that the prepared compounds would possess anti-inflammatory activity. The anti-inflammatory activity of the hybrids was screened using RAW 264.7 stimulated by LPS. First, the ability of compounds to affect the proliferation of the cells was tested at 25 μM using an MTT assay. All tested AKBA hybrids were found to be noncytotoxic to the RAW 264.7 or HepG2 cell line at such a concentration, as presented in Table 1

2.2.1.2. Effect of Hybrids on Nitric Oxide (NO) Levels. Based on the obtained data from the preliminary cytotoxicity assay, the ability of AKBA hybrids to downregulate NO production in RAW 264.7 induced by LPS was assessed at a concentration of 10 μM, as an elevated level of nitric oxide is an important marker for inflammation. Eleven hybrids achieved better inhibition of NO than the parent compound. Eight of them showed better activity when compared to L-NG-nitro arginine methyl ester (L-Name), a known standard inhibitor of NO with a percent inhibition of more than 85%. Interestingly, three of them were AKBA−thymol conjugates with different linkers, while the other conjugates were menthol, 2,5-benzaldehyde, 3,4,5-trimethoxy benzaldehyde, isovanillin, and isatin, with percent inhibition up to 91% (Table 2).

2.2.1.3. Gene Expression of TNF-α Using Real-Time PCR. The above finding prompted us to evaluate the ability of the most active hybrids to modulate the gene expression of TNF-α using real-time PCR. All of the compounds were able to downregulate TNF-α in comparison to cells treated with LPS, but thymol **5b** and isatin **18** conjugates were able to exhibit a threefold decrease in the gene expression, which is comparable activity to the standard dexamethasone, as shown in Figure 2a. Therefore, compounds **5b** and **18** were selected for further investigation to assess their ability to attenuate APAP-induced inflammation in HepG2.

Table 1. Cytotoxicity of AKBA Hybrids to RAW 264.7 and HepG2[a]

no.	compound	viability % RAW 264.7 at 25 μM	HepG2 at 25 μM
1	**1**	92 ± 1.2	86 ± 2.6
2	14a	89 ± 1	85 ± 0.55
3	**14b**	100 ± 1.2	93 ± 0.38
4	**14c**	103 ± 0.6	94 ± 0.18
5	**16a**	92 ± 1	92 ± 1
6	**16b**	85 ± 45	90 ± 0.95
7	**16c**	86 ± 1.5	94 ± 2
8	**16d**	95 ± 1.7	87 ± 1.7
9	**16e**	94 ± 0.7	93 ± 2.4
10	**16f**	95 ± 2.8	99 ± 0.61
11	**16g**	98 ± 0.56	88 ± 0.45
12	**16h**	92 ± 0.3	90 ± 0.69
13	**16i**	99 ± 0.9	89 ± 2.1
14	**16j**	102 ± 2.6	91 ± 0.76
15	**18**	99 ± 0.9	93 ± 1.7
16	**2a**	95 ± 1.5	96 ± 1.5
17	**2b**	98 ± 0.7	93 ± 1.2
18	**5a**	93 ± 0.9	90 ± 1.2
19	**5b**	88 ± 1.3	91 ± 1.2
20	**5c**	84 ± 2.4	86 ± 1.3
21	**5d**	96 ± 0.8	104 ± 2.8
22	**8a**	99 ± 1.5	99 ± 1.5
23	**8b**	104 ± 0.7	95 ± 0.23
24	**8c**	99 ± 3	87 ± 0.25

[a]Mean ± SD of % viability of two independent experiments.

Table 2. Nitric Oxide Inhibition in RAW 264.7 Induced by LPS after Treatment of AKBA Hybrids at 10 μM[a]

no.	compound	no. inhibition %
1	**1**	74 ± 0.1
2	**3a**	82.52 ± 1.15
3	**3b**	82.07 ± 0.65
4	**5a**	75.34 ± 1.39
5	**5b**	89.69 ± 0.43
6	**5c**	66.37 ± 1
7	**5d**	69.51 ± 2.41
8	**8a**	74.44 ± 0.8
9	**8b**	85.21 ± 2.41
10	**8c**	76.24 ± 3.52
11	**14a**	88.35 ± 2.26
12	**14b**	85.66 ± 0.68
13	**14c**	62.79 ± 2.06
14	**16a**	59.2 ± 0.15
15	**16b**	89.69 ± 0.78
16	**16c**	68.61 ± 2.29
17	**16d**	96.42 ± 0.27
18	**16e**	64.58 ± 1.93
19	**16f**	67.72 ± 1.94
20	**16g**	70.86 ± 2.12
21	**16h**	85.21 ± 0.69
22	**16i**	80.72 ± 1.57
23	**16j**	84.31 ± 2.05
24	**18**	91.04 ± 0.62
25	L-NAME[b]	84.76 ± 0.4

[a]Mean ± SD of % viability of two independent experiments. [b]Concentration at 250 μM.

https://doi.org/10.1021/acsomega.3c05247
ACS Omega 2023, 8, 39490−39510

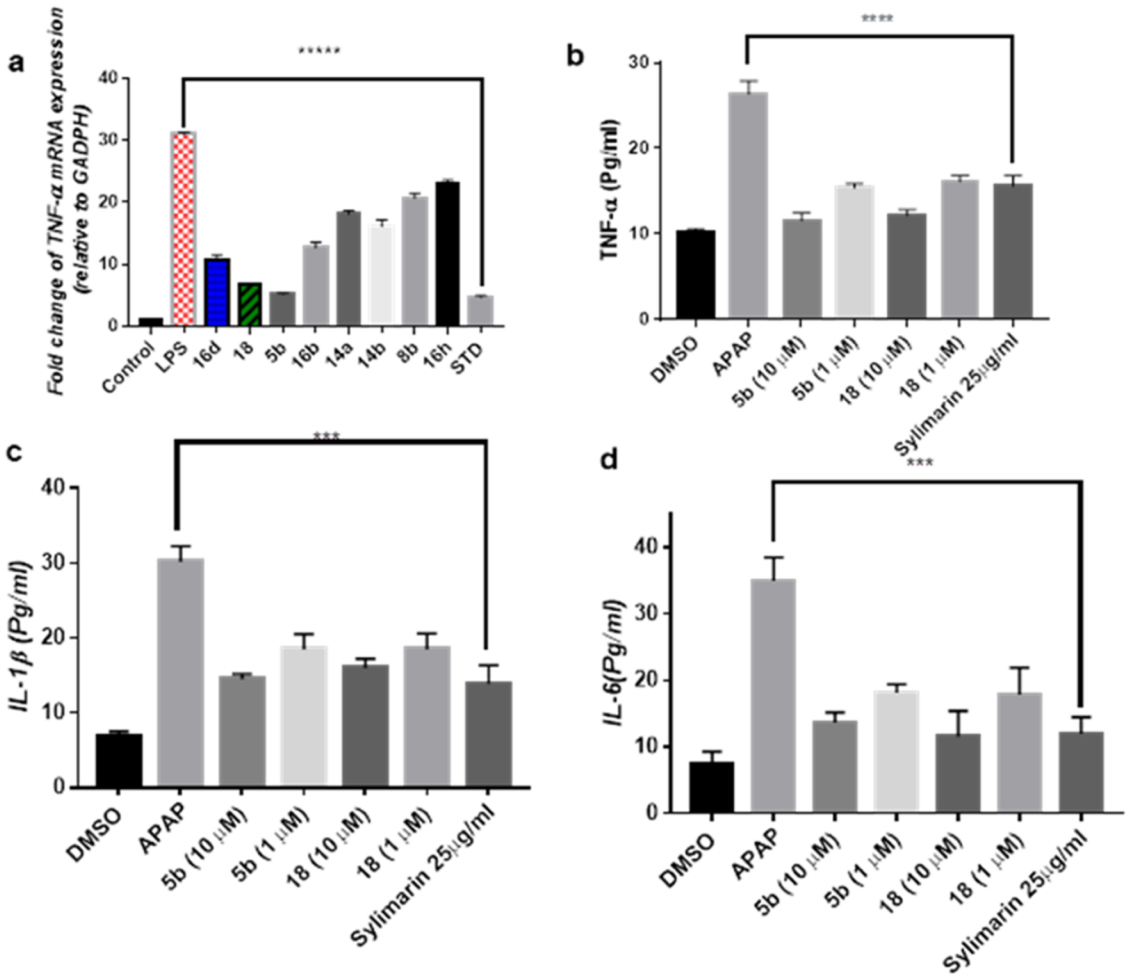

Figure 2. Effect of compounds **5b** and **18** on (A) gene expression of TNF-α in comparison to standard dexamethasone in RAW 264.7 stimulated by LPS. (B) TNF-α levels, (C) IL-1β, and (D) IL-6 in HepG2 in the presence of 10 m MAPAP in comparison to silymarin. *** represents a significant difference from the control group at $p < 0.0005$. ***** represents a significant difference from the control group at $p < 0.0001$.

2.2.1.4. APAP Induced Inflammation in HepG2. All of the experiments were carried out at 1 μM and 10 μM, whereas both concentrations proved to be nontoxic to HepG2 cells. The production of different cytokines such as TNF-α, IL-6, and IL-1β was measured as APAP-treated cells showed a significant increase in comparison to nontreated cells. Compounds **5b** and **18** decreased TNF-α production by approximately 56 and 54%, respectively, at a dose of 10 μM. On the other hand, compounds **5b** and **18** lowered TNF-α levels by approximately 41 and 39%, respectively, compared to APAP-treated cells when treated with a dose of 1 μM.

In the case of IL-6, at a dose of 10 μM, compounds **5b** and **18** reduced IL-6 by approximately 61 and 67%, respectively, while at a dose of 1 μM, compounds **5b** and **18** reduced IL-6 production by approximately 67 and 48%, respectively, compared to APAP. On the other hand, silymarin decreased IL-6 production by approximately 66% compared to APAP. Finally, for Il-1β, it was found that at 10 μM, compounds **5b** and **18** reduced IL-1β production by approximately 52 and 47%, respectively. While at dose 1 μM, both compounds **5b** and **18** decreased IL-1β levels by approximately 39%. This indicated that both compounds **5b** and **18** were able to regulate cytokine production to normal levels in a dose-dependent manner, which is comparable to 25 μg/mL silymarin, a known standard hepatoprotective compound (Figure 2b–d).

2.2.2. Estimation of Oxidative Stress Markers: Reduced Glutathione (GSH), Superoxide Dismutase (SOD) Level, and Malondialdehyde (MDA). Having the anti-inflammatory properties of compounds **5b** and **18** been proven, their ability to regulate oxidative stress markers such as reduced glutathione (GSH), superoxide dismutase level (SOD), and malondialdehyde (MDA) was assessed. APAP-treated cells showed a significant decrease in SOD and GSH, while MDA levels were increased. On the contrary, treatment of the cells with compound **5b** led to an increase of SOD levels from 31 U/mg in APAP-treated cells to 73 and 64 at 10 and 1 μM, respectively.

Whereas, compound **18** increased SOD to 78 and 72 at 10 and 1 μM, respectively, which is comparable to the effect of standard silymarin. Also, in the case of GSH, treatment with compound **5b** at 10 and 1 μM resulted in increases in GSH levels to 6.3 and 5.2, respectively, compared to APAP-treated cells. Similarly, treatment with compound **18** at 10 and 1 μM increased GSH levels to 7.2 and 6.3, respectively, which was comparable to the effect of silymarin.

Treatment with APAP led to a significant increase in MDA (18.5 nmol/mg), which was reversed when compound **5b** was added at 10 or 1 μM in combination with APAP, where the

https://doi.org/10.1021/acsomega.3c05247
ACS Omega 2023, 8, 39490−39510

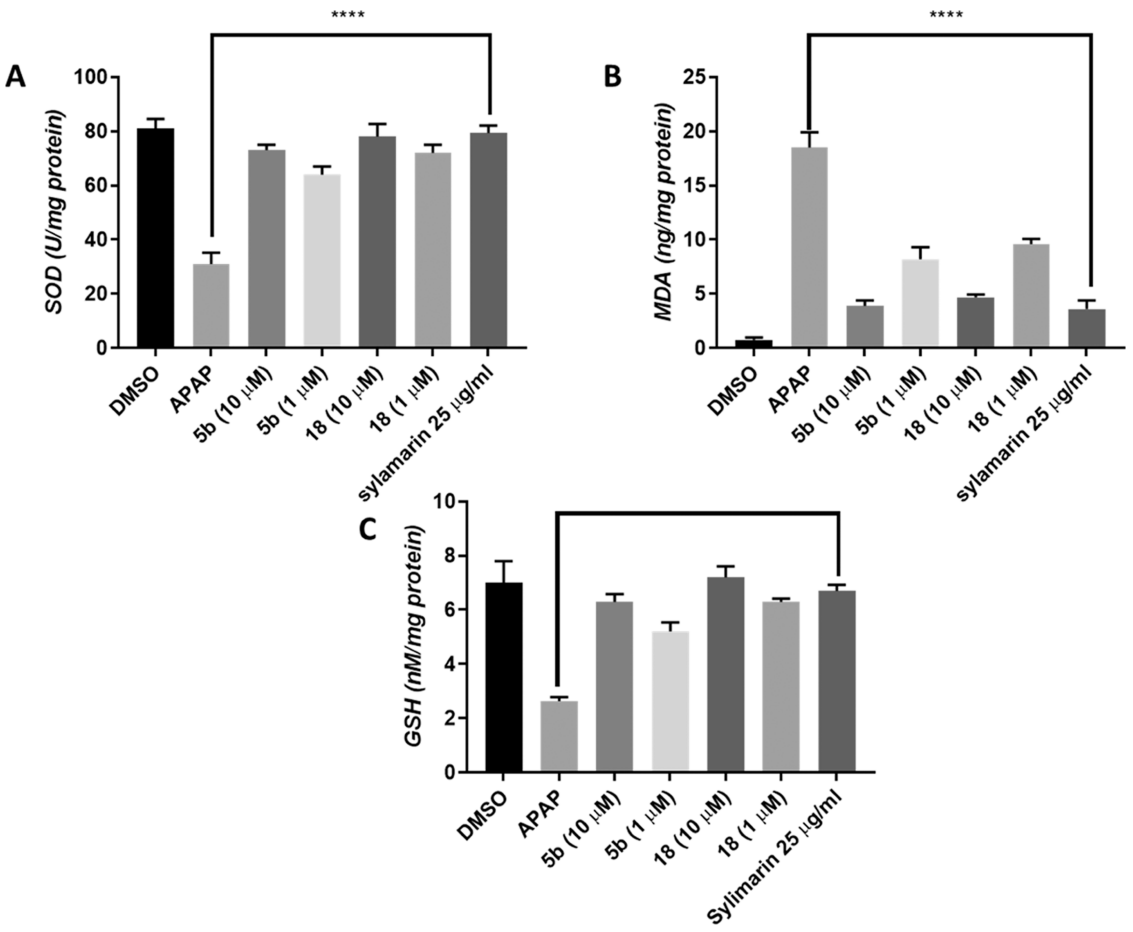

Figure 3. Effect of compounds **5b** and **18** on antioxidant markers, (A) SOD, (B) GSH, and (C) MDA, in comparison to standard silymarin on APAP-induced hepatotoxicity in HepG2.**** represents a significant difference from the control group at $p < 0.0005$.

levels of MDA decreased to 3.9 and 8.2 nmol/mg, respectively. Also, compound **18** at 10 and 1 μM led to a decrease of MDA levels to 4.7 and 9.6 nmol/mg, respectively. Again, this was similar to the effect exerted by silymarin treatment, which decreased MDA levels to 3.6 nmol/mg (Figure 3a–c).

In light of these findings, AKBA–thymol and AKBA–isatin were able to regulate several molecular targets associated with APAP-induced hepatitis in a dose-dependent manner, achieved better activity than the parent compound, and were comparable to known anti-inflammatory and hepatoprotective agents. This is in accordance with previous studies reporting the potential use of triterpenes in the management of hepatic-related pathogenesis and their ability to restore a normal hepatic environment.[34]

For example, boswellic acids showed a prominent *in vivo* hepatoprotective effect against APAP-induced hepatotoxicity in mice by modulating inflammatory and oxidative stress markers.[35] This was also supported by the ability of boswellic acid combinations to protect against acute liver injury induced by galactosamine/endotoxin by targeting TNF-α.[36] Another important factor to consider is the ability of AKBA to inhibit 5-lipooxygenase (5-LOX), which was reported to help in the reduction of hepatic damage.[37,38] Also, boswellic acid was identified as a promising agent in prevention of nonalcoholic fatty acid,[39] hepatic steatosis,[40] polycyclic aromatic hydrocarbon-induced liver injury in a rat model,[15] and doxorubicin-induced hepatotoxicity.[41]

For the counterpart of the hybrid **5b**, thymol, there are uncountable studies addressing its anti-inflammatory and antioxidant effect, which revealed its ability to affect a plethora of pathological pathways associated with hepatotoxicity.[42] Interestingly, these effects were proven to be reproducible in different models studying liver injury where thymol was able to protect against ethanol-induced hepatotoxicity through decreasing nitric oxide release and preventing autophagy;[43] also, it attenuated LPS-induced hepatitis in mice by preventing NLRP3 inflammasome activation and mTOR and AMPK pathways.[44]

Moreover, thymol was found to possess a hepatoprotective effect against thioacetamide-induced hepatic encephalopathy in rats by the downregulation of NF-$\kappa\beta$ and normalization of hepatic enzymes.[45] More importantly, at a dose of 100 μM, thymol ameliorated APAP hepatotoxicity in HepG2,[46] showing the ability of the prepared hybrid to exert better activity compared to thymol alone, which could be explained by its ability to target multiple pathways involved in hepatotoxicity.

In the case of compound **18**, isatin was the conjugate with AKBA. It is a unique natural product isolated from *Isatis tinctoria* with diverse biological activities and was found to be one of the oxidation metabolites of indole by cytochrome p450.[47,48] It was reported to show anti-inflammatory and antioxidant effects in different experimental models, and several analogues were designed for such purpose. These bioactivities were attributed to its ability to downregulate proinflammatory and ROS generation mechanisms.[49−51]

https://doi.org/10.1021/acsomega.3c05247
ACS Omega 2023, 8, 39490−39510

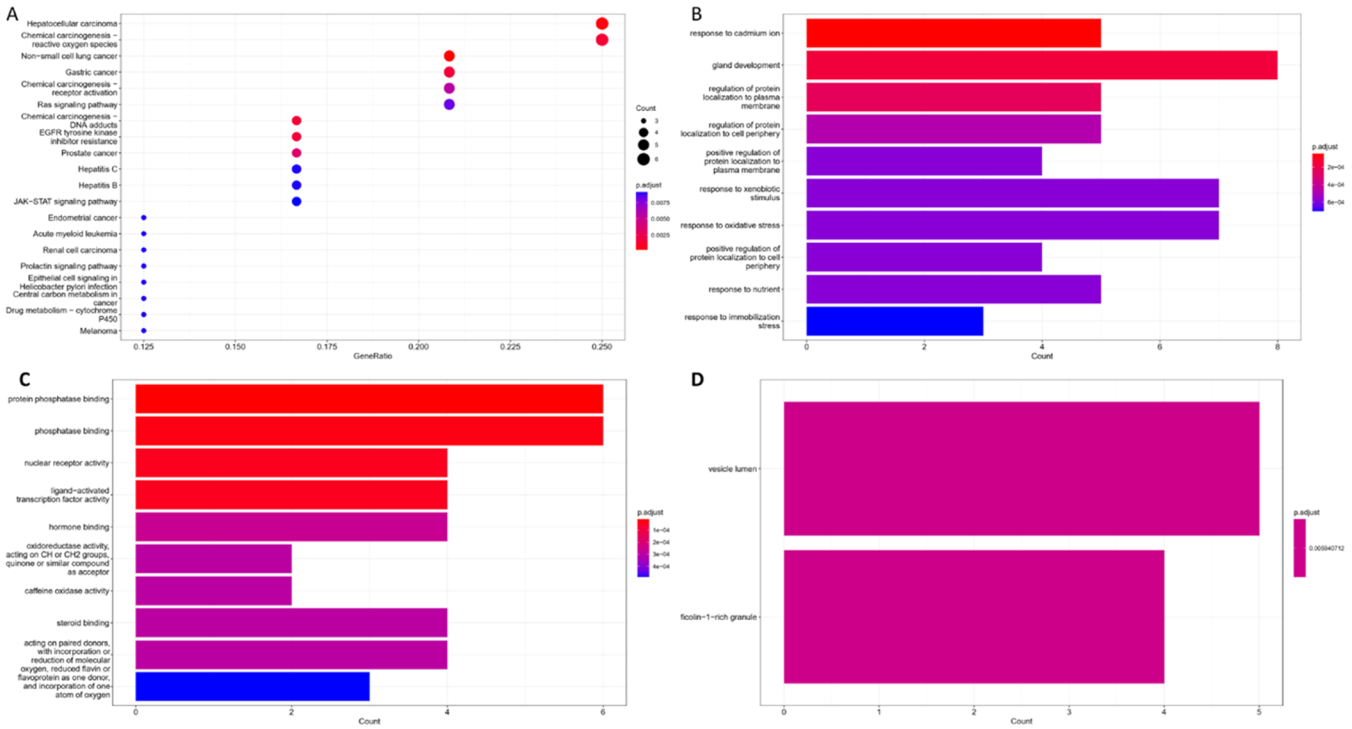

Figure 4. Enrichment analysis of terms related to hepatitis and targets associated with AKBA hybrid activity. (A) KEGG, (B) biological processes, (C) molecular functions, and (D) cellular components.

In this context, isatin hydrazone derivatives demonstrated a hepatoprotective effect against carbon tetrachloride in rats.[52] Recently, isatin was found to prevent carcinogenesis in the liver induced by diethyl nitrosamine (DENA) in rats by the upregulation of the Nrf2 signaling pathway, which led to a decrease in the levels of several proinflammatory markers such as TNF-α, IL-1β, and IL-6,[53] which verify our findings and justify the better activity of the AKBA−isatin conjugate over other hybrids.

2.3. *In Silico* Evaluation of Most Active Hybrids. *2.3.1. Network Pharmacology.* The multifaceted nature of drug-induced hepatitis requires the regulation of several molecular pathways involved in its pathogenesis. Hence, it is logical to utilize pharmacological agents with multitherapeutic activities. As previously established, AKBA conjugates exhibited substantial anti-inflammatory and hepatoprotective effects in APAP-induced hepatotoxicity, so network pharmacology analysis was performed to get insights into different molecular, biological, and cellular processes that might be correlated with the observed activity.

For such a purpose, target prediction using Pharmmaper and Swiss target prediction server revealed 438 potential targets of the prepared hybrids; among them, 28 targets related to hepatitis were retrieved and subjected to enrichment analysis using Gene Ontology (GO) annotation and KEGG to identify different BP, MF, and CC related to hepatitis.

Interestingly, top biological processes that are significantly enriched were related to hepatic cancer and chemical carcinogenesis related to reactive oxygen species, as shown in Figure 4a; also, the epidermal growth factor receptor, phosphoinositide 3-kinase (PI3K), was significantly highlighted as the main targets involved in these processes. This agrees with reports indicating that the regulation of these targets plays an important role in the management of APAP hepatotoxicity and liver injury-related conditions, for example, EGFR activation has been noticed in the early stages of APAP-induced injury, which led to the initiation of liver repair mechanisms[18,54]

More importantly, PI3K is regulated as part of the downstream signaling pathway of EGFR; hence, the emergence of PI3K among the enriched targets is not surprising. In fact, the regulation of PI3K was suggested by many studies as a potential mechanism for abrogation of APAP toxicity.[55,56] It is worth noting that the ability of several triterpenes similar to boswellic acids to interact with this target is reported.[57,58] Moreover, thymol, which is part of the hybrid **5b**, was reported to protect against xenobiotic-induced injury by the regulation of PI3K-related pathways.[44,45,59]

Also, enriched terms in BP were a response to a cadmium ion, gland development, and the regulation of protein localization to the plasma membrane and cell periphery at $p = 0.0002$ and a response to xenobiotic and oxidative stress at $p = 0.0004$, as demonstrated in Figure 4b. All of these terms are related to reactive oxygen species, oxidative stress, and inflammation, which would eventually lead to the distribution of the cellular function of liver glands and impairing repairing mechanisms. Change in the localization of some proteins, such CYP2E1, has been proposed as an adapting response to drug-induced liver injury, especially in the case of APAP.[60] This mechanism was mimicked by boswellic acid as it was able to reduce the levels of CYP2E1 in a dose-dependent manner in an alcoholic liver induced experimentally.[61]

For MF, protein phosphatase, phosphatase binding, hormone binding, nuclear receptor activity, and ligand-activated transcription factor activity were among the top five enriched MF at $p = 0.0004$, as depicted in Figure 4c. This could be supported by previous studies explaining the role of protein phosphatase and physiological protein phosphorylation in the development of APAP toxicity.[62] Nevertheless, the inhibition of phosphorylation of several inflammatory proteins,

https://doi.org/10.1021/acsomega.3c05247
ACS Omega 2023, 8, 39490−39510

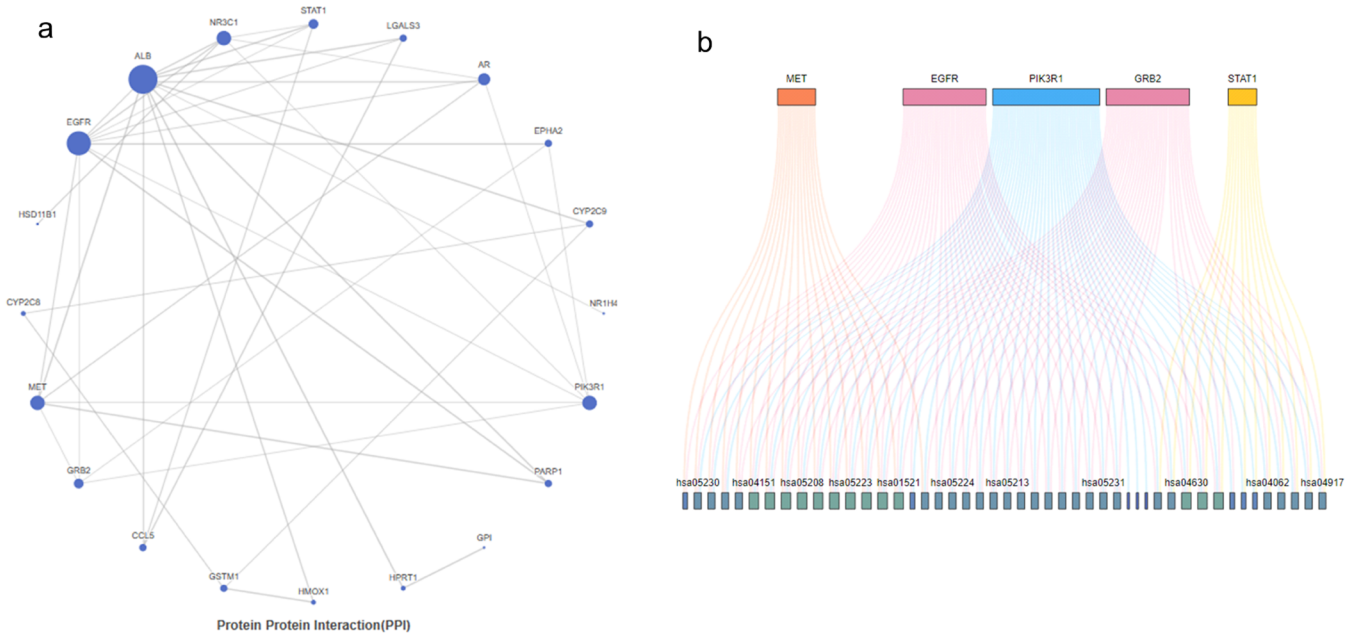

Figure 5. (A) Protein−protein interaction network constructed from the most relevant targets associated with the activity of the AKBA hybrid. (B) Top five pathways identified in the KEGG. The visualization of the gene−pathway relationships using colored lines illustrates the extensive overlap and interconnectivity between these pathways.

such as mitogen-activated protein kinases, could also be a potential MF as they are well known for their contribution to oxidative stress and liver injury.

In this context, the anti-inflammatory mechanism of boswellic acids was attributed to their ability to downregulate the phosphorylation of p38 MAPK, NF-KB, and JNK.[35,63] Finally, vesicle lumen and ficolin 1-rich granule CC terms were significantly enriched (p = 0.005), as shown in Figure 4d.

These elements play an important role in the activation liver's immune response to mitigate the damage and initiate repair processes.[64,65] As the enrichment of ficolin 1-rich granules may indicate a specific immune response associated with hepatotoxicity, targeting innate immunity responses has been investigated to control APAP-related toxicity.[66] There are no previous data addressing the ability of the prepared hybrids or their components to directly regulate this marker; still, the ability of boswellic acids to modulate innate immunity in different tissues has been proven.[67−69]

To obtain more information about other pathways involved in the hepatoprotective effect of the prepared hybrids, a protein−protein interaction network was constructed where interactions were filtered based on a confidence score threshold of 0.7 to ensure reliable interactions in our network. Again, EGFR and PI3K appear to be responsible for most of the interactions followed by GRB2, MET, and STAT1, as demonstrated in Figure 5a,b and Table S24. Nevertheless, PI3K was shown to be the most significant target as it was involved in interaction with 45 out of 54 targets enriched from KEGG related to hepatitis, while EGFR interacted with 35 of 54.

2.3.2. Molecular Docking. Since PI3K emerged as the most promising target for the most active hybrids, we used molecular docking to identify their potential interaction with this target. First, putative active sites were recognized by the CB-Dock2 server, as there were no previous reports about the binding mode of AKBA to PI3K. Three binding sites were detected, so molecular docking was performed, and the two hybrids were ranked according to their binding energy. Since both compounds showed remarkable binding affinity to active site number 1 (Table 3), their poses were selected for postdocking analysis.

Table 3. Blind Docking Results of the AKBA Hybrid in Different Binding Sites in the PI3K Complex

binding site	cavity volume (Å^3)	docking size (X,Y,Z)	center box (X,Y,Z)	Vina score of **18**	Vina score of **5b**
1	32,498	75,51,81	35,35,35	−11.4	−10.6
2	7532	66,79,91	35,27,35	−9.0	−10.1
3	3805	90,79,92	27,27,27	−7.8	−8.4

Unexpectedly, both of the compounds did not interact with the ATP active site; instead, the best binding site was recognized between the interface of the catalytic p110α and the regulatory subunit p85α complex, probably due to its relatively large cavity volume and the ability of both compounds to form several hydrogen bonds and hydrophobic interactions with the active site. Still, compound **18** showed better binding energy as it formed hydrogen bonds with Gly451, His450, Tyr467, and ASN457 through the acetyl group and carbonyl of AKBA and Thr679 and Ile459 with the amide functionality in the isatin moiety; also, it formed hydrophobic interactions with Trp446, Pro447, Lys678, and Gly1009, as shown in Figure 6a,b.

Whereas, in the case of compound **5b**, it interacted with His450, Asn465, Asn457, and Arg808 through hydrogen bonding with the acetyl and carbonyl functionality in the AKBA scaffold and with Lys640 through the acetyl linker between AKBA and thymol. Moreover, it formed hydrophobic interactions with Val461, Pro447, Tyr556, Asn677, Lys678, and Thr679, as depicted in Figure 6c,d. This binding mode suggests the ability of AKBA hybrids to mitigate APAP-induced hepatotoxicity by disrupting protein−protein inter-

https://doi.org/10.1021/acsomega.3c05247
ACS Omega 2023, 8, 39490−39510

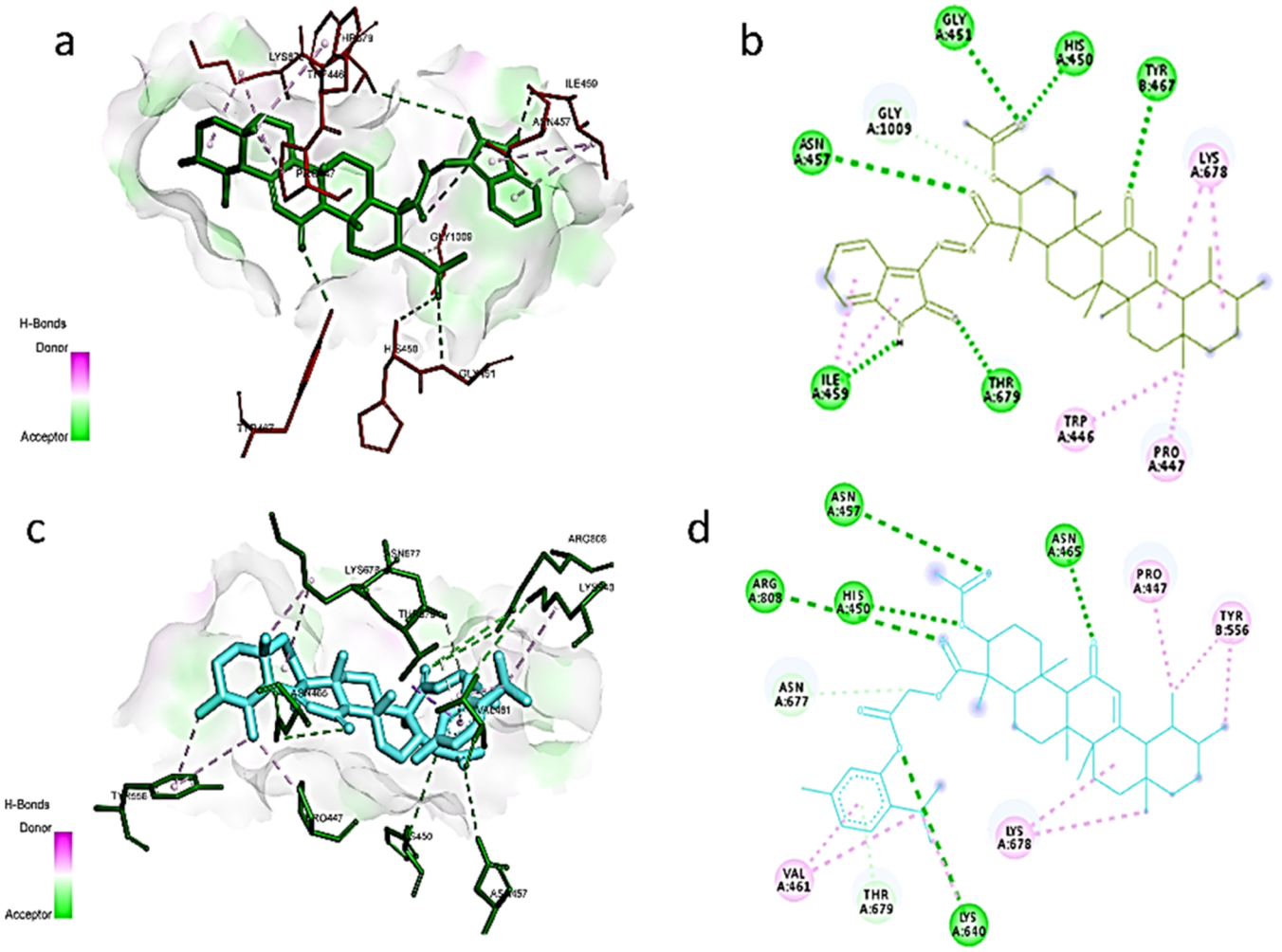

Figure 6. (A) 3D interaction of compound **18** (green) with site-1 in the PI3K complex (PDB: 3HNM). (B) 2D interaction of compound **18** (green) with site-1 in the PI3K complex. (C) 3D interaction of compound **5b** (cyan) with site-1 in the PI3K complex (PDB: 3HNM). (D) 2D interaction of compound **18** (cyan) with site-1 in the PI3K complex.

Table 4. ADMET Prediction of the Most Active Hybrids

	compound **5b**		compound **18**	
ADMET	PreADMET server	PkCSM server	PreADMET server	PkCSM server
intestinal absorption	97.83%	100%	96.0%	100%
volume of distribution (human) (log L/kg)	0.916	−0.331	1.137	−0.404
skin permeability log Kp, cm/h	−0.72	−2.73	−1.83944	−2.749
P-glycoprotein I inhibitor	yes	yes	yes	yes
cytochrome P450 inhibition	no	no	no	no
excretion log mL/min/kg		−0.508		−0.555
Ames test	nonmutagen	nonmutagen	nonmutagen	nonmutagen
hepatotoxicity	no	no	no	no

action between the p110α and p85α complex (Figure S1), which would consequently block the inhibitory action of p85α,[70] leading to the activation of PI3k signaling, which was reported as a promising approach in the management of APAP liver injury.[56,71,72]

2.3.3. ADMET Assessment of Compounds ***5b*** *and* ***18****.* ADMET prediction has been extensively used to obtain insights about the pharmacokinetic properties of drug-like compounds.[73,74] In the case of compound **5b**, both predicted values in the PkCSM server and PreADMET showed that human intestinal absorption was 100 and 97.83%, respectively. The compounds showed a reasonable volume of distribution and skin permeability. Both servers showed that the compound is a potential inhibitor for p-glycoprotein but does not affect the cytochrome p450 system. Additionally, the PkCSM server showed that the excretion rate of the compound is in the safe range. Regarding the toxicity profile, both servers showed that the compound is neither mutagenic nor hepatotoxic. Moreover, ProTOX-II predicted that compound 5b is relatively safe with LD_{50} = 2000 mg/kg.

For compound **18**, the PkCSM server and PreADMET predicted that human intestinal absorption was 100 and 96%,

https://doi.org/10.1021/acsomega.3c05247
ACS Omega 2023, 8, 39490−39510

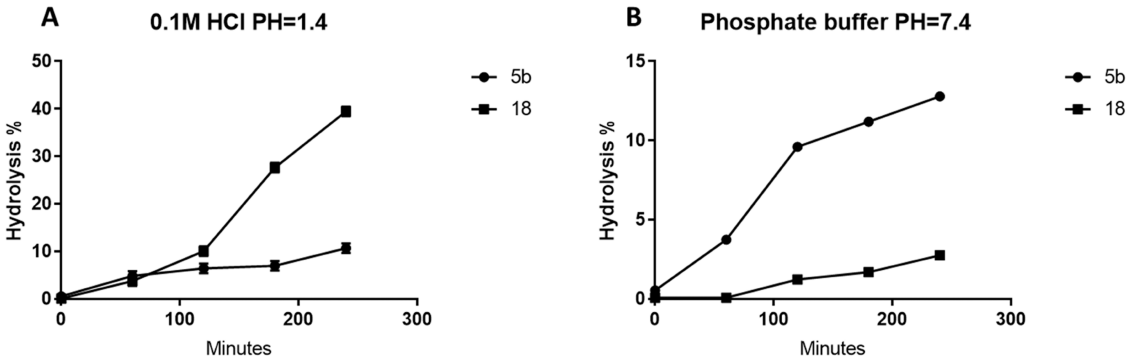

Figure 7. Preliminary stability studies of the hybrids **5b** and **18** at (A) pH = 1.4 and (B) phosphate buffer pH = 7.4. Data were derived from three independent experiments as mean ± SD.

respectively. The compounds showed a good volume of distribution and skin permeability. Both servers revealed its ability to inhibit p-glycoprotein but not the cytochrome p450 system. Furthermore, the PkCSM server showed that the excretion rate of the compound is in the safe range. Again, toxicity prediction showed that the compound is neither mutagenic nor hepatotoxic. Moreover, ProTOX-II predicted that compound **18** is potentially safe with LD_{50} = 1400 mg/kg. The ADMET prediction results are shown in Tabe 4.

2.4. Preliminary Stability Studies. Since compounds **5b** and **18** showed better activity than other hybrids, we decided to investigate their stability in conditions simulating gastric and intestinal environments. At 0.1 M HCl, compound **5b** showed excellent stability with $t_{1/2}$ equal to 25.3 h. In contrast, the $t_{1/2}$ of compound **18** was 5.74 h, as demonstrated in Figure 7a. This situation was reversed at pH = 7.4; since compound **5b** is ester, it was more labile to hydrolysis than compound **18**, where their $t_{1/2}$ values were 20.9 h and 4.6 days, respectively, as shown in Figure 7b. This is in agreement with previous studies indicating that hydrazones have lower stability in an acidic medium rather than basic or neutral conditions, while esters tend to act as prodrugs in relatively basic pH, leading to a continuous release of the active substrate. Nevertheless, esters have substantial resistance to acid hydrolysis.[75,76] Still, the obtained data infer that the gastric or intestinal environment might not affect the absorption of both compounds since they showed reasonable stability in both acidic and slightly basic environments.

3. CONCLUSIONS

In this study, we successfully prepared 23 novel conjugates of AKBA and other natural products. Among them, AKBA−thymol and AKBA−isatin were able to reduce cytokine production in the RAW 264.7 cell line induced by LPS and remarkably alleviated the hepatotoxic effects of APAP in the HepG2 cell line by exerting anti-inflammatory activity and boosting the levels of antioxidant enzymes such as GSH and SOD and decreasing MDA levels. The regulation of PI3K by AKBA hybrids was suggested as a possible mechanism of action. This was supported by their ability to interact with the active site lying between the interface of catalytic p110α and the regulatory subunit p85α complex, as shown by molecular docking study. This would eventually prevent the inactivation of p110α by the p85α complex, leading to the activation of PI3K and related downstream pathways promoting cell survival and tissue regeneration. The stability of the most active hybrids in simulated gastric and intestinal pH suggested that they would probably be absorbed unchanged. Finally, the combination of AKBA, thymol, or isatin through chemical hybridization could unleash their multitherapeutic potential as a promising approach to manage complex conditions such as APAP toxicity and other related disorders. Full detailed kinetic studies are needed before clinical application can be established.

4. MATERIALS AND METHODS

4.1. Chemistry. *4.1.1. General.* Melting point equipment (FALC, Italy) was used to record the melting point. A Bruker spectrometer at 400 MHz for ^{1}H NMR and 101 MHz ^{13}C NMR was used to collect NMR spectra in deuterated dimethyl sulfoxide (DMSO) or chloroform $CDCl_3$. Chemical shifts (δ) were recorded relative to the solvent (DMSO) or $CDCl_3$ as parts per million (ppm). The reported coupling constant (J) are in hertz. Mass spectra were obtained utilizing a mass spectrometer: Thermo scientific ISQLT single quadrupole. Elemental analysis for C, H, N, and S was done utilizing a PerkinElmer 240, and all results were found within the accepted limits. Commercially available solvents and reagents were used without further purification.

4.1.2. Isolation and Purification of AKBA. The isolation of AKBA **1** was performed as previously mentioned, and it was obtained as white needles and confirmed with cochromatography with standard AKBA provided by F. A. Badria.[77]

*4.1.3. Synthesis of AKBA Hybrid Esters (**3a−b**).* AKBA **1** (102.55 mg, 0.2 mmol), 1-ethyl-3-(3-(dimethylamino)propyl)-carbodiimide (EDCI) (38.81 mg, 0.25 mmol), and 4-dimethylaminopyridine (DMAP) (2.44 mg, 0.02 mmol) in anhydrous methylene chloride (DCM) (25 mL) were mixed for 10 min in an ice salt bath. This was followed by addition of the corresponding alcohol/phenol **2a-b** (0.2 mmol) dropwise over a period of 1 h with continuous stirring, at the same temperature; finally, the reaction mixture was left to stir further 48 h at room temperature. Once the reaction was completed, it was filtered and evaporated *in vacu*. Flash chromatography was used for purification where gradient elution from 100 to 70% in a petroleum ether:ethyl acetate mobile phase allowed obtaining compounds **3a-b in** pure form.

*4.1.3.1. Menthyl(3-acetoxy-11-oxo-12-ursen-24-oate) (**3a**).* Yield 25%; ^{1}H NMR (400 MHz, $CDCl_3$) δ ppm: 5.6 (s, 1H, CH═C-AKBA), 5.2 (s, 1H, CH−O−AKBA), 4.6 (td, J = 11.3, 4.0 Hz, 1H, CH−O−AKBA), 4.4 (dd, J = 11.8, 4.7 Hz, 1H, CH−O−menthol), 2.7 (d, J = 13.5 Hz, 1H, CH−AKBA), 2.3 (s, 1H, AKBA), 2.0 (d, J = 13.0 Hz, 1H, menthol), 1.9 (t, J = 14.3 Hz, 3H, AKBA), 1.8 (d, J = 15.3 Hz, 2H, menthol), 1.7

https://doi.org/10.1021/acsomega.3c05247
ACS Omega 2023, 8, 39490−39510

(dd, J = 14.2, 4.1 Hz, 1H, menthol), 1.6 (q, J = 10.4, 8.8 Hz, 5H), 1.5 (d, J = 14.4 Hz, 2H), 1.5−1.4 (m, 1H), 1.3 (d, J = 8.7 Hz, 8H), 1.3−1.2 (m, 1H), 1.1 (s, 3H), 1.1 (s, 6H), 1.0 (p, J = 12.1, 11.3 Hz, 4H), 0.9−0.8 (m, 5H), 0.8 (s, 8H, 2(CH_3−menthol), 0.7 (d, J = 10.1 Hz, 4H, menthol−CH_3), 0.7 (d, J = 7.0 Hz, 6H); ^{13}C NMR (101 MHz, $CDCl_3$) δ ppm: 200.2 (C═O), 175.9 (O═C−CH_3), 171.1 O═C−CH_3), 169.6 (CH═AKBA), 128.5 (C═CH), 80.6 (CH−O−menthol), 76.7 (CH−O−AKBA), 74.2, 61.7, 55.0, 48.4, 47.0, 46.9, 45.4, 44.0, 43.3, 41.1, 40.9, 38.9, 38.8, 38.0, 37.7, 37.0, 34.2, 32.7, 31.8, 31.5, 31.2, 28.7, 28.3, 28.0, 26.4, 26.1, 23.6, 22.0, 21.3, 20.8, 18.7, 17.4, 16.7, 16.4, 15.9; displayed a molecular ion at m/z 650.49 calculated for the molecular formula anal. calcd for $C_{42}H_{66}O_5$: C, 77.49; H, 10.22; found C, 77.93; H, 10.03.

*4.1.3.2. Thymyl(3-acetxoy-11-oxo-12-ursen-24-oate) (**3b**).* Yield 15%; 1H NMR (400 MHz, CDCl3) δ ppm: 7.5 (t, J = 7.7 Hz, 1H), 7.4−7.3 (m, 2H), 5.5 (s, 1H), 5.4 (d, J = 3.0 Hz, 1H), 2.6 (dt, J = 13.5, 3.6 Hz, 1H), 2.4 (s, 1H), 2.3−2.2 (m, 2H), 2.1 (s, 3H), 1.9 (q, J = 4.7 Hz, 3H), 1.7−1.6 (m, 2H), 1.6−1.5 (m, 1H), 1.5 (d, J = 11.1 Hz, 6H), 1.4 (d, J = 3.0 Hz, 1H), 1.3 (d, J = 8.7 Hz, 12H), 1.2 (d, J = 13.4 Hz, 8H), 1.0−0.9 (m, 2H), 0.9 (d, J = 4.6 Hz, 5H), 0.8−0.7 (m, 8H); 13C NMR (101 MHz, CDCl3) δ ppm: 198.9 (C═O), 172.3 (O═C−CH_3), 170.0 (O═C−CH_3), 165.3 (CH═AKBA), 143.5 (C−O Ar−thymol), 130.4 (Ar−thymol), 128.9 (C═CH), 128.7 (Ar−thymol), 124.9 (Ar−thymol), 120.6 (Ar−thymol), 116.0 (Ar−thymol), 72.2 (CHO−AKBA), 60.2, 59.1, 50.6, 47.2, 45.1, 43.8, 40.9, 39.4, 39.3, 37.4, 34.2, 34.0, 32.7, 30.9, 28.9, 27.5, 27.2, 23.8, 23.6, 22.7, 21.3, 21.2, 20.6, 19.0, 18.4, 17.4, 14.2; displayed a molecular ion at m/z 644.44 calculated for the molecular formula anal. calcd for $C_{42}H_{60}O_5$ C: 78.22; H, 9.38; found C, 78.68; H, 9.53.

*4.1.4. Synthesis of Bromoacetyl Derivatives (**4a−d**).* Acetyl derivatives were prepared using the previously reported method[27] to obtain compounds (**4a−d**)

*4.1.5. Synthesis of the AKBA Hybrid Acetyl Linker Derivative (**5a−d**).* Bromoacetate derivatives **4a−d** (0.20 mmol), AKBA 1 (102.55 mg, 0.2 mmol), potassium carbonate (41.5 mg, 0.3 mmol), and potassium iodide (3.32 mg, 0.02 mmol) in DMF (10 mL) was prepared. This mixture was stirred for 48 h at room temperature. Crushed ice was added to the reaction mixture while stirring and then extracted with ethyl acetate (3 × 25 mL). The ethyl acetate layer was dried over anhydrous sodium sulfate and removed under reduced pressure to obtain a semisolid residue. This residue was chromatographed using gradient elution from 100 to 70% using petroleum ether:ethyl acetate as a mobile phase to obtain compounds **5a−d**.

*4.1.5.1. 2-Menthoxyl-2-oxoethyl 2-(3-acetxoy-11-oxo-12-ursen-24-oate) (**5a**).* Yield 20%; ^{1}H NMR (400 MHz, $CDCl_3$) δ ppm: 5.5 (s, 1H, C═CH−AKBA), 5.3 (d, J = 2.9 Hz, 1H, CH−O−AKBA), 4.7 (dt, J = 10.9, 5.5 Hz, 1H, CHO−menthol), 4.6 (d, J = 15.8 Hz, 1H, CH−C═O), 4.5 (d, J = 15.8 Hz, 1H, CH−C ═ O), 2.5 (dt, J = 13.3, 3.6 Hz, 2H), 2.1 (ddd, J = 17.9, 9.5, 3.3 Hz, 1H), 2.0 (s, 4H), 1.9−1.7 (m, 3H), 1.7−1.5 (m, 4H), 1.5−1.3 (m, 10H), 1.3 (s, 5H), 1.2 (s, 3H), 1.1 (s, 4H), 1.0 (s, 4H), 1.0−0.9 (m, 2H), 0.9 (s, 4H), 0.8 (t, J = 6.2 Hz, 8H), 0.8−0.7 (m, 6H), 0.7 (d, J = 6.8 Hz, 3H); ^{13}C NMR (101 MHz, $CDCl_3$) δ ppm: 199.3 (C═O), 175.1 (OC═O), 170.2 (OC═O), 167.2 (CH_2−C═O−linker), 165.0 (olefinic), 130.5 (olefinic), 75.6 (CHO−menthol), 73.2 (CHO−AKBA), 60.8, 60.3, 59.0, 50.4, 46.9, 46.8, 45.1, 43.8, 40.9, 40.7, 39.3, 39.3, 37.3, 34.6, 34.1, 34.0, 32.9, 31.4, 30.9, 28.9, 27.5, 27.2, 26.1, 23.9, 23.5, 23.3, 22.0, 21.4, 21.2, 20.8, 20.6, 18.8, 18.3, 17.4, 16.2, 13.4; displayed a molecular ion at m/z 708.49 calculated for the molecular formula anal. calcd for $C_{44}H_{68}O_7$: C, 74.54; H, 9.67; found C, 75.04; H, 10.0.

*4.1.5.2. 2-Thymoxyl-2-oxoethyl 2-(3-acetoxy-11-oxo-12-ursen-24-oate) (**5b**).* Yield 15%; ^{1}H NMR (400 MHz, $CDCl_3$) δ ppm: 7.1 (d, J = 7.9 Hz, 1H, aromaic), 7.0 (dd, J = 8.0, 1.7 Hz, 1H, Ar−H), 6.7 (d, J = 1.8 Hz, 1H, Ar−H), 5.5 (s, 1H, olefinic), 5.3 (d, J = 2.9 Hz, 1H, CHO−AKBA), 4.9 (d, J = 16.0 Hz, 1H, CH−C═O), 4.8 (d, J = 16.0 Hz, 1H, CH−C═O), 2.9−2.8 (m, 1H), 2.5 (dt, J = 13.2, 3.6 Hz, 3H), 2.4 (s, 1H), 2.2 (ddd, J = 17.8, 9.5, 3.9 Hz, 1H), 2.0 (s, 4H), 1.8 (dtd, J = 24.5, 13.4, 4.0 Hz, 2H), 1.7−1.7 (m, 1H), 1.6 (ddq, J = 15.5, 10.5, 3.8 Hz, 2H), 1.4 (dd, J = 20.5, 8.1 Hz, 2H), 1.4 (dt, J = 12.2, 4.1 Hz, 4H), 1.3 (s, 4H), 1.2−1.1 (m, 7H), 1.1−1.1 (m, 9H), 1.0 (s, 3H), 1.0−0.9 (m, 1H), 0.9 (s, 4H), 0.8−0.7 (m, 6H); ^{13}C NMR (101 MHz, $CDCl_3$) δ ppm: 199.4 (C═O), 175.1 (OC═O), 170.3 (OC═O), 166.6 (CH_2−C═O−linker), 165.2 (olefinic), 147.1 (Ar−C−O), 137.0, 136.8, 130.5 (olefinic), 127.6, 126.6, 122.4, 73.2, 60.5, 59.0, 50.4, 46.8, 45.1, 43.8, 40.9, 39.3, 39.3, 37.3, 34.5, 34.0, 32.9, 30.9, 28.9, 27.5, 27.2, 27.0, 23.9, 23.6, 23.1, 23.1, 21.4, 21.2, 20.8, 20.5, 18.8, 18.3, 17.4, 13.5; displayed a molecular ion at m/z 702.44 calculated for the molecular formula anal. calcd for $C_{44}H_{62}O_7$: C, 75.18; H, 8.89; found C, 75.63; H, 8.55.

*4.1.5.4. 2-Vanillyl-2-oxoethyl 2-(3-acetoxy-11-oxo-12-ursen-24-oate) (**5c**).* Yield 8%; ^{1}H NMR (400 MHz, $CDCl_3$) δ ppm: 9.8 (s, 1H, CHO−vanillin), 7.4 (dd, J = 5.9, 1.9 Hz, 2H, Ar−H), 7.1 (d, J = 8.5 Hz, 1H, Ar−H), 5.6 (s, 1H, olefinic), 5.4 (d, J = 2.8 Hz, 1H, CH−O), 4.8 (d, J = 16.2 Hz, 1H, CH−CO−linker), 4.6 (d, J = 16.2 Hz, 1H, CH−CO−linker), 4.0 (s, 3, OCH_3), 2.6−2.5 (m, 1H), 2.4 (d, J = 2.5 Hz, 1H), 2.2 (s, 2H), 2.1 (d, J = 2.0 Hz, 4H), 1.9 (td, J = 10.0, 8.8, 3.5 Hz, 2H), 1.8−1.6 (m, 4H), 1.6 (d, J = 11.0 Hz, 1H), 1.5−1.4 (m, 4H), 1.4 (s, 1H), 1.3 (d, J = 8.7 Hz, 5H), 1.2 (d, J = 2.9 Hz, 4H), 1.2 (s, 1H), 1.1 (d, J = 9.9 Hz, 2H), 1.0 (dd, J = 14.0, 4.6 Hz, 1H), 1.0 (s, 5H), 0.9−0.8 (m, 7H); ^{13}C NMR (101 MHz, $CDCl_3$) δ ppm: 199.6 (C═O), 191.1 (CHO−vanillin), 175.0 (OC═O), 170.4 (OC═O), 165.4 (2c), (olefinic and CH_2−C═O−linker), 151.8 (Ar−OCH_3), 147.2 (Ar−OH), 130.4 (olefinic), 129.8, 127.7, 114.4, 108.8, 73.2, 60.3, 59.0, 56.1, 50.4, 46.8, 46.5, 45.1, 45.1, 43.8, 40.9, 39.3, 39.3, 37.3, 34.5, 34.0, 32.9, 30.9, 28.9, 27.5, 27.2, 23.9, 23.6, 21.4, 21.2, 20.5, 18.7, 17.4, 13.4; displayed a molecular ion at m/z 704.39 calculated for the molecular formula anal. calcd for $C_{42}H_{56}O_9$: C, 71.56; H, 8.01; found C, 71.95; H, 8.15.

*4.1.5.3. 2-Eugenyl-2-oxoethyl 2-(3-acetoxy-11-oxo-12-ursen-24-oate) (**5d**).* Yield 12%; ^{1}H NMR (400 MHz, $CDCl_3$) δ ppm: 6.9 (d, J = 7.9 Hz, 1H, Ar−H), 6.7−6.6 (m, 2H, Ar−H), 5.9 (ddt, J = 16.9, 10.2, 6.7 Hz, 1H, olefinic−eugenol), 5.5 (s, 1H, olefinic−AKBA), 5.3 (d, J = 2.9 Hz, 1H, CH−O−AKABA), 5.1−5.0 (m, 1H, olefinic−eugenol), 5.0−5.0 (m, 1H, olefinic−eugenol), 4.9 (d, J = 16.0 Hz, 1H CH−CO−linker), 4.8 (d, J = 16.0 Hz, 1H, CH−CO−linker), 3.7 (s, 3H, OCH_3), 3.3 (d, J = 6.8 Hz, 2H, CH_2−C═C−eugneol), 2.5 (dt, J = 13.0, 3.5 Hz, 1H), 2.3 (s, 1H), 2.2 (td, J = 14.2, 13.0, 3.5 Hz, 1H), 2.0 (s, 3H), 1.9−1.7 (m, 4H), 1.7−1.5 (m, 2H), 1.5−1.4 (m, 1H), 1.4 (ddd, J = 12.1, 10.0, 7.2 Hz, 4H), 1.2 (d, J = 31.6 Hz, 9H), 1.2 (s, 2H), 1.1 (d, J = 4.1 Hz, 0H), 1.1 (s, 3H), 1.0 (s, 3H), 1.0−0.9 (m, 1H), 0.9 (s, 4H), 0.8−0.7 (m, 6H); ^{13}C NMR (101 MHz, $CDCl_3$) δ ppm: 199.4 (C═O), 175.0, 170.2 (OC═O), 165.9 (olefinic−AKBA), 165.0

https://doi.org/10.1021/acsomega.3c05247
ACS Omega 2023, 8, 39490−39510

(CH_2−C═O−linker), 150.6 (Ar−OCH_3), 139.5, 137.2 (olefinic−eugenol), 137.0, 130.5 (olefinic−AKBA), 122.3, 120.7, 116.3 (olefinic−eugenol), 112.8, 73.2, 60.4, 60.3, 59.0, 55.9, 50.4, 46.8, 45.1, 43.8, 40.9, 40.1, 39.3, 39.3, 37.3, 34.5, 34.0, 32.9, 30.9, 28.9, 27.5, 27.2, 23.9, 23.6, 21.4, 21.2, 20.6, 18.8, 18.3, 17.4, 13.4; displayed a molecular ion at m/z 716.42 calculated for the molecular formula anal. calcd for $C_{44}H_{60}O_8$: C, 73.71; H, 8.44; found C, 73.25; H, 9.03.

*4.1.6. Synthesis of the AKBA Hybrid Oxadiazole Linker (**8a−c**).* **AKBA 1** (0.51 g, 1 mmol) was subjected to reflux in 25 mL of thionyl chloride for 4 h. The solution was then evaporated *in vacu*. Next, the crude products were transformed into the corresponding ester by adding isopropanol (25 mL) and stirring for 0.5 h. Finally, the corresponding hydrazide **6** was obtained by refluxing the reaction mixture with 20 mL of 95% hydrazine hydrate for 3 h. After cooling, the formed precipitate was filtered under a vacuum and washed with cold isopropanol to give an off-white powder (mp = 207−210 °C).

The prepared hydrazide **6** (0.58 g, 1.1 mmol) and potassium hydroxide (0.067 g, 1.2 mmol) were stirred in absolute ethanol (25 mL), and then carbon disulfide (0.5 mL) was added. The reaction mixture was subjected to reflux for 6 h. The reaction mixture was left to cool and chilled water was poured onto it; then, dilute hydrochloric acid (10%) was added, leading to precipitation of the 1,3,4-oxadiazole derivative of AKBA **7**, which was filtered under pressure to obtain an off-white powder (mp = 270−273 °C).

1,3,4-Oxadiazole derivative **7** (73.95 mg, 0.13 mmol) was mixed with **4a-b** and **4d** (0.14 mmol), and potassium carbonate (27.64 mg, 0.2 mmol) in DMF (5 mL) and stirred for 24 h at room temperature. Crushed ice was added to the mixture while stirring; ethyl acetate (3 × 25 mL) was used for extraction and removed under reduced pressure to obtain the crude products as compounds **8a−c**. Compounds **8a−c** were purified by column chromatography using gradient elution from 100 to 60% in a petroleum ether:ethyl acetate mobile phase.

*4.1.6.1. Menthol2-((5-((3-acetoxy-11-oxo-12-ursen-24-yl))-1,3,4-oxadiazol-2-yl)thio)acetate (**8a**).* Yield 30%; ^{1}H NMR (400 MHz, $CDCl_3$) δ ppm: 5.5 (s, 1H, (s, 1H, C═CH)AKBA), 4.7 (td, J = 10.9, 4.4 Hz, 1H, CH−O−AKBA), 4.3 (d, J = 2.9 Hz, 1H, CH−O−menthol), 4.0 (s, 2H CH−C═O−linker), 2.5−2.4 (m, 3H), 2.0 (td, J = 13.7, 4.8 Hz, 1H), 1.9 (dd, J = 11.8, 4.4 Hz, 4H), 1.9−1.7 (m, 3H), 1.6 (tdd, J = 13.4, 9.5, 3.0 Hz, 6H), 1.5−1.3 (m, 7H), 1.3 (d, J = 16.8 Hz, 8H), 1.2−1.1 (m, 3H), 1.1 (s, 3H), 1.0−0.9 (m, 4H), 0.9−0.8 (m, 12H), 0.8−0.7 (m, 6H), 0.7 (d, J = 6.9 Hz, 3H); ^{13}C NMR (101 MHz, $CDCl_3$) δ ppm: 199.3 (C═O), 172.2 (C, OC═O), 167.0 (CH_2−C═O−linker, C═N−oxadiazole), 165.1 (C, olefinic-−AKBA), 162.2 (C═N−oxadiazole), 130.4 (olefinic−AKBA), 76.7 (CHO−AKBA), 70.6 (CHO−menthol), 60.3, 59.0, 53, 49.2, 46.9, 45.0, 43.8, 41.9, 40.9, 40.6, 39.3, 37.1, 34.7, 34.1, 34.0, 33.7, 32.7, 31.4, 30.9, 28.9, 27.5, 27.2, 26.2, 26.0, 25.4, 23.3, 22.0, 21.2, 20.8, 20.6, 18.6, 18.4, 17.5, 16.2, 13.1; displayed a molecular ion at m/z 764.47 calculated for the molecular formula anal. calcd for $C_{45}H_{68}N_2O_6S$: C, 70.64; H, 8.96; N, 3.66; S, 4.19; found C, 70.79; H, 9.23; N, 3.44; S, 4.46.

*4.1.6.2. Thymol-2-((5-((3-acetoxy-11-oxo-12-ursen-24-yl))-1,3,4-oxadiazol-2-yl)thio)acetate (**8b**).* Yield 25%; ^{1}H NMR (400 MHz, $CDCl_3$) δ ppm: 7.2 (d, J = 7.9 Hz, 1H, AROMAIC), 7.1 (dd, J = 7.9, 1.7 Hz, 1H, Ar−H), 6.9 (d, J = 1.8 Hz, 1H, Ar−H), 5.5 (s, 1H, olefinic), 5.3 (s, 1H, CHO−AKBA), 4.3 (d, J = 4.1 Hz, 2H, CH_2−C═O−linker), 3.0 (hept, J = 6.9 Hz, 1H, CH−thymol), 2.6−2.5 (m, 2H), 2.5 (s, 1H), 2.3 (s, 3H), 2.1 (td, J = 13.7, 4.8 Hz, 1H), 1.9−1.8 (m, 2H), 1.7 (td, J = 15.8, 13.4, 7.5 Hz, 9H), 1.6−1.4 (m, 6H), 1.4 (d, J = 22.0 Hz, 9H), 1.2 (d, J = 6.9 Hz, 7H), 1.1 (s, 3H), 1.1−1.0 (m, 2H), 1.0 (s, 5H), 0.8−0.8 (m, 7H), 0.7 (s, 3H); ^{13}C NMR (101 MHz, $CDCl_3$) δ ppm: 199.2 (C═O), 172.4 (2C, OC═O), 166.5 (2C, CH_2−C═O−linker, C═N−oxadiazole), 165.1 (olefinic), 161.9 (C═N−oxadiazole), 147.6 (Ar−C−O)136.9, 136.8, 130.4 (olefinic), 127.6, 126.6, 122.3, 70.7, 60.3, 59.0, 53.47 49.2, 45.0, 43.8, 42.0, 40.9, 39.3, 37.1, 34.4, 34.0, 33.7, 32.7, 30.9, 28.9, 27.5, 27.2, 27.0, 26.1, 25.4, 23.1, 23.1, 21.2, 20.8, 20.6, 18.6, 18.3, 17.5, 13.1; displayed a molecular ion at m/z 758.43 calculated for the molecular formula anal. calcd for $C_{45}H_{62}N_2O_6S$: C, 7.21; H, 8.23; N, 3.69; S, 4.22; found C, 6.76; H, 7.65; N, 4.10; S, 4.35.

*4.1.6.3. Eugenol2-((5-((3-acetoxy-11-oxo-12-ursen-24−25yl))-1,3,4-oxadiazol-2-yl)thio)acetate (**8c**).* Yield 20%; ^{1}H NMR (400 MHz, $CDCl_3$) δ ppm: 7.0 (d, J = 7.9 Hz, 1H, Ar−H), 6.8−6.7 (m, 2H, Ar−H), 6.0 (ddt, J = 15.6, 10.5, 6.7 Hz, 1H, olefinic−eugenol), 5.5 (s, 1H, olefinic−AKBA), 5.3 (s, 1H, CH−O−AKBA), 5.2−5.1 (m, 2H, CH_2═CH, olefinic−eugenol), 4.3 (d, J = 1.5 Hz, 2H, CH−CO−linker), 3.8 (s, 3H, OCH_3′), 3.4 (d, J = 6.7 Hz, 2H, 2H, CH_2−C═C), 2.6−2.5 (m, 2H), 2.5 (s, 1H), 2.1 (td, J = 13.7, 4.9 Hz, 1H), 1.9−1.8 (m, 2H), 1.7 (qd, J = 12.2, 6.3 Hz, 9H), 1.5 (dd, J = 16.2, 2.2 Hz, 2H), 1.4 (s, 4H), 1.3 (s, 4H), 1.3−1.2 (m, 1H), 1.1 (s, 3H), 1.0 (dd, J = 12.2, 3.6 Hz, 1H), 1.0 (s, 5H), 0.8−0.8 (m, 7H), 0.7 (s, 3H); ^{13}C NMR (101 MHz, $CDCl_3$) δ ppm: 199.3 (C═O), 172.3 (2C, OC═O), 165.9 (2C, CH_2−C═O−linker, C═N−oxadiazole), 165.1 (olefinic−AKBA), 162.0 (C═N−oxadiazole), 150.5 (Ar−OCH_3), 139.6, 137.7 (olefinic−eugenol), 136.9, 130.4 (olefinic−AKBA), 122.2, 120.7, 116.3 (olefinic−eugenol), 112.7, 70.7, 60.3, 59.0, 55.8, 53.0, 49.2, 45.0, 43.8, 42.0, 40.9, 40.1, 39.3, 37.1, 34.3, 34.0, 33.7, 32.7, 30.9, 28.9, 27.5, 27.2, 26.1, 25.4, 21.2, 20.6, 18.6, 18.3, 17.5, 13.1; displayed a molecular ion at m/z 772.41 calculated for the molecular formula anal. calcd for $C_{45}H_{60}N_2O_7S$: C, 69.92; H, 7.82; N, 3.62; S, 4.15; found C, 69.42; H, 7.53; N, 3.71; S, 3.97.

*4.1.7. Synthesis of Azide Derivatives (**9a-b and 12**).* The bromoacetate derivatives **4a-b** were used to prepare the corresponding azide. **4a-b** (2 mM) and sodium azide (3 mM) were dissolved in a solution of ethanol/water (1:1) for 3 h. Upon the completion of the reaction, the solvent was removed *in vacu* and extracted with ethyl acetate (3 × 25 mL). Anhydrous sodium sulfate was used to ensure the removal of water traces from the organic layer, which was removed under pressure to get an oily liquid, which was utilized without further processing to obtain **9a-b**.

For coumarin azide preparation, phosphorus oxychloride (20 mL) was added to **10** (8 mM); after that, triethylamine (12 mmol) was added dropwise, and the reaction was subjected to reflux for 4 h. Once completed, distillation was used to remove phosphorus oxychloride excess. The crude product was obtained as a yellowish brown residue, but crystallization from petroleum ether yielded white needles of 4-chloro coumarin **11** with an mp range of 85−87 °C (reported mp = 84−86 °C[78]).

Intermediate **11** (3 mM) and sodium azide (4.5 mM) were stirred at room temperature for 5 h in dry acetone. Once completed, the solvent was removed under pressure, dissolved in 50 mL of water, and partitioned with ethyl acetate (3 × 25

https://doi.org/10.1021/acsomega.3c05247
ACS Omega 2023, 8, 39490−39510

mL). The ethyl acetate layer was dried over anhydrous sodium sulfate and removed under pressure to give white needles of **12** with an mp range of 160−163 °C (reported mp = 165−167 °C[79]).

*4.1.8. Synthesis of the AKBA Hybrid with the 1,2,3-Triazole Linker (**14a−c**).* AKBA **1** (1 mM) and potassium carbonate (1 mM) were mixed in DMF for 20 min, followed by the addition of propargyl bromide (1 mM), and the reaction was stirred at room temperature for 3 h. Based on TLC, reaction progress was monitored until completion, and then crushed ice was added with stirring. The aqueous solution of the reaction was extracted with ethyl acetate (3 × 25 mL), which was rendered dry using anhydrous sodium sulfate, and then removed *in vacu* to get the crude product. Recrystallization from methanol was enough to obtain **13** as pure white needles.

Sodium ascorbate (1.2 equiv) and copper sulfate pentahydrate (1.2 equiv) in water were stirred with **13** (0.1 mM) in DMF. After the addition of different azide derivatives **9a-b** or **12** (1.1 equiv) to the reaction, it was allowed to stir at room temperature for 48 h. Crushed ice was added to the reaction upon its completion. The crude product was extracted with ethyl acetate (3 × 25 mL), which was removed under pressure. Pure compounds **14a−c** were obtained by column chromatography using gradient elution from 100 to 60% in a methylene chloride:ethyl acetate mobile phase.

*4.1.8.1. (1-(2-(Menthoxy)-2-oxoethyl)-1H-1,2,3-triazol-5-yl)methine-3-acetoxy-11-oxo-12-ursen-24-oate (**14a**).* Yield 20%; ^{1}H NMR (400 MHz, $CDCl_3$) δ ppm: 7.8 (s, 1*H*-triazole), 5.6 (s, 1H, C═CH, AKBA), 5.4−5.2 (m, 3H, menthol−OCH and CH_2−C═O−linker), 5.2 (s, 1H, AKBA−OCH), 3.7 (q, *J* = 7.0 Hz, 2H.CH_2−C═O−linker), 2.5 (dt, *J* = 13.3, 3.4 Hz, 1H), 2.4 (s, 1H), 2.1 (s, 3H), 2.0−1.7 (m, 4H), 1.7 (s, 5H), 1.6−1.4 (m, 5H), 1.5−1.3 (m, 9H), 1.3−1.1 (m, 6H), 1.2 (d, *J* = 4.7 Hz, 5H), 1.1−1.0 (m, 3H), 1.0−0.9 (m, 12H), 0.9 (d, *J* = 3.4 Hz, 1H), 0.9−0.8 (m, 6H), 0.8 (d, *J* = 6.9 Hz, 3H); ^{13}C NMR (101 MHz, $CDCl_3$) δ ppm: 199.3 (C═O), 175.6 (OC═O), 170.2 (OC═O), 165.5 (olefinic−AKBA), 165.1 (CH_2−C═O−linker), 130.5 (2C, C═N-triazole and olefinic−AKBA), 125.7 (C═N-triazole), 73.2 (CH−O−menthol), 60.2, 59.0, 58.5, 57.4, 51.1, 50.5, 46.8, 46.7, 45.0, 43.8, 40.9, 40.6, 39.3, 39.3, 37.2, 34.5, 34.0, 32.8, 31.4, 30.9, 28.8, 27.5, 27.2, 26.3, 23.7, 23.6, 23.3, 21.9, 21.4, 21.2, 20.7, 20.5, 18.8, 18.5, 18.3, 17.4, 16.3, 13.2; displayed a molecular ion at *m*/*z* 789.52 calculated for the molecular formula anal. calcd for $C_{47}H_{71}N_3O_7$: C, 71.45; H, 9.06; N, 5.32; found C, 71.06; H, 9.19; N, 5.19.

*4.1.8.2. (1-(2-(Thymoxy)-2-oxoethyl)-1H-1,2,3-triazol-5-yl)methyl-3-acetoxy-11-oxo-12-ursen-24-oate (**14b**).* Yield 17%; ^{1}H NMR (400 MHz, $CDCl_3$) δ ppm: 7.8 (s, 1H, 1*H*-triazole), 7.1 (d, *J* = 8.0 Hz, 1H, Ar−H), 7.0 (d, *J* = 8.0 Hz, 1H, Ar−H), 6.8 (s, 1H, Ar−H), 5.5 (s, 1H, AKBA−olefinic), 5.4 (s, 2H, CH_2−C═O−linker), 5.2 (q, *J* = 6.6, 5.9 Hz, 3H CH_2−C═O, CH−O−AKBA), 2.8 (hept, *J* = 6.8 Hz, 1H, CH−thymol), 2.4 (dd, *J* = 13.5, 3.6 Hz, 2H), 2.3 (d, *J* = 7.5 Hz, 2H), 2.2 (s, 3H), 2.2−2.0 (m, 3H), 2.0 (s, 3H), 1.8−1.7 (m, 5H), 1.3 (s, 4H), 1.1−1.1 (m, 3H), 1.1−1.1 (m, 10H), 1.0 (s, 3H), 1.0−0.9 (m, 2H), 0.9 (s, 5H), 0.8 (s, 3H), 0.8−0.7 (m, 6H); ^{13}C NMR (101 MHz, $CDCl_3$) δ ppm: 199.3 (C═O), 175.6 (OC═O), 170.2 (OC═O), 165.1 (olefinic−AKBA), 164.8 (CH_2−C═O−linker), 147.1 (Ar−thymol), 143.0 (C═N-triazole), 137.0 (Ar), 136.7 (Ar), 130.4 (olefinic−AKBA), 127.9 (Ar), 126.7 (Ar), 125.6 (C═N-triazole), 122.1 (Ar), 73.2, 60.2, 59.0, 57.4, 50.9, 50.5, 46.7, 45.0, 43.7, 40.9, 39.3, 39.3, 37.2, 34.5, 34.0, 32.8, 30.9, 28.9, 27.5, 27.2, 27.2, 23.7, 23.6, 23.0, 21.4, 21.2, 20.8, 20.5, 18.8, 18.2, 17.4, 13.2; displayed a molecular ion at *m*/*z* 783.48 calculated for the molecular formula anal. calcd for $C_{47}H_{65}N_3O_7C$: 72.0; H, 8.36; N, 5.36; found C, 71.90; H, 8.18; N, 5.81.

*4.1.8.3. (1-(2-Oxo-2H-chromen-4-yl)-1H-1,2,3-triazol-5-yl)methyl-3-acetoxy-11-oxo-12-ursen-24-oate (**14c**).* Yield 22%; ^{1}H NMR (400 MHz, $CDCl_3$) δ ppm: 8.0 (s, 1H, 1*H*-triazole), 7.7 (dd, *J* = 8.2, 1.5 Hz, 1H, Ar−H), 7.7−7.6 (m, 1H, Ar−H), 7.4 (d, *J* = 8.2 Hz, 1H, Ar−H), 7.3 (t, *J* = 7.7 Hz, 1H, Ar−H), 6.5 (s, 1H, olefinic−coumarin), 5.5 (s, 1H, olefinic−AKBA), 5.3 (s, 2H, CH_2−C═O−linker), 5.3−5.2 (m, 1H, CH−O−AKBA), 2.4 (d, *J* = 3.5 Hz, 1H), 2.4 (t, *J* = 3.6 Hz, 1H), 2.3 (s, 1H), 2.3−2.0 (m, 2H), 2.0 (s, 3H), 1.7−1.6 (m, 2H), 1.6−1.4 (m, 5H), 1.4−1.3 (m, 6H), 1.2 (t, *J* = 3.6 Hz, 1H), 1.1 (d, *J* = 14.6 Hz, 6H), 1.1 (s, 3H), 1.0−0.9 (m, 2H), 0.9 (d, *J* = 14.6 Hz, 7H), 0.8−0.7 (m, 5H); ^{13}C NMR (101 MHz, $CDCl_3$) δ ppm: 199.2 (C═O), 175.6 (OC═O), 170.2 (OC═O), 165.2 (olefinic−AKBA), 159.6 (C═O−umbelliferone), 154.3 (2C, olefinic−coumarin, Ar), 146.6 (C═N-triazole), 133.8 (Ar), 130.4 (olefinic−AKBA), 125.3 (C═N-triazole), 125.2 (Ar), 117.7 (Ar), 114.3 (Ar), 110.3 (olefinic−coumarin), 73.0 (CH−O−AKBA), 60.1, 59.0, 57.0, 50.5, 46.8, 45.0, 43.8, 40.9, 39.3, 39.3, 37.2, 34.5, 34.0, 32.7, 30.9, 28.9, 27.5, 27.2, 23.8, 23.6, 21.4, 21.2, 20.5, 18.8, 18.3, 17.4, 13.3; displayed a molecular ion at *m*/*z* 737.4 calculated for the molecular formula anal. calcd for $C_{44}H_{55}N_3O_7$: C, 71.62; H, 7.51; N, 5.69; found C, 71.86; H, 7.25; N, 5.60.

*4.1.9. Synthesis of the AKBA Hybrid with the Hydrazone Linker (**16a−j**).* Compound **6** (0.05 mM) in absolute ethanol was mixed with proper aldehydes **15a−j** or isatin **17** (0.05 mM) in the presence of glacial acetic acid (catalytic amount). The mixture was subjected to reflux for 1−2 h. Once completed, the reaction solvent was removed under a vacuum and subjected to column chromatography using gradient elution from 100 to 70% in a petroleum ether:ethyl acetate mobile phase to obtain **16a−j** and **18**.

*4.1.9.1. E-3-Acetoxy-11-oxo-12-ursen-24-oic Acid-Benzylidene Hydrazide (**16a**).* Yield 30% mp = 190−193 °C ^{1}H NMR (400 MHz, $CDCl_3$) δ ppm: 8.7 (s, 1H, NH−N═C), 8.2 (s, 1H, CH═N of a hydrazone linker), 7.6 (dd, *J* = 6.7, 3.0 Hz, 2H, Ar−H), 7.3−7.3 (m, 3H, Ar−H), 5.5 (s, 1H, olefinic−AKBA), 4.2 (s, 1H, CH−O−AKBA), 2.5 (dq, *J* = 12.5, 5.2, 4.4 Hz, 1H), 2.4 (d, *J* = 8.5 Hz, 2H), 2.0 (dd, *J* = 13.5, 4.8 Hz, 1H), 2.0 (dd, *J* = 7.9, 3.5 Hz, 1H), 1.8 (tt, *J* = 20.0, 9.1 Hz, 4H), 1.6−1.3 (m, 7H), 1.3 (s, 4H), 1.3 (s, 4H), 1.2 (d, *J* = 4.7 Hz, 1H), 1.2−1.1 (m, 8H), 1.0−0.9 (m, 1H), 0.9 (s, 4H), 0.8−0.7 (m, 7H); ^{13}C NMR (101 MHz, $CDCl_3$) δ ppm: 199.2 (C═O), 173.39 (2C, C═OO), 165.0 (olefinic−AKBA), 147.8 (CH═N), 133.7 (Ar), 130.5 (olefinic−AKBA), 130.0 (Ar), 4, 129.8 (Ar), 129.0 (Ar), 128.7 (Ar), 127.6 (Ar), 70.3 (CH−O−AKBA), 60.5, 59.0, 49.0, 47.5, 45.1, 43.8, 40.9, 39.3, 37.6, 34.2, 34.0, 33.2, 30.9, 29.7, 28.9, 27.5, 27.2, 26.6, 24.7, 21.1, 20.5, 19.9, 18.3, 17.5, 13.8; displayed a molecular ion at *m*/*z* 614.9 calculated for the molecular formula anal. calcd for $C_{39}H_{54}N_2O_4$: C, 76.18; H, 8.85; N, 4.56; found C, 76.02; H, 9.10; N, 4.15.

*4.1.9.2. E-3-Acetoxy-11-oxo-12-ursen-24-oic Acid-2,5-Dimethoxy Benzylidene Hydrazide (**16b**).* Yield 40%, mp = 225−228 °C ^{1}H NMR (400 MHz, $CDCl_3$) δ ppm: 8.9 (s, 1H, NH═N of a hydrazone linker,), 8.5 (s, 1H, hydrazone linker), 7.6 (d, *J* = 3.1 Hz, 1H, Ar−H), 6.9 (dd, *J* = 9.1, 3.1 Hz, 1H,

https://doi.org/10.1021/acsomega.3c05247
ACS Omega 2023, 8, 39490−39510

Ar−H), 6.8 (d, J = 9.1 Hz, 1H, Ar−H), 5.5 (s, 1H, olefinic−AKBA), 4.2 (s, 1H, CH−O−AKBA), 3.8 (s, 3H−OCH_3), 3.8 (s, 3H−OCH_3), 2.6−2.4 (m, 3H), 2.1−2.0 (m, 2H), 1.9−1.7 (m, 5H), 1.6−1.4 (m, 7H), 1.3 (d, J = 21.2 Hz, 8H), 1.3−1.1 (m, 9H), 1.0 (dd, J = 13.3, 4.4 Hz, 1H), 0.9 (s, 5H), 0.8−0.8 (m, 6H); ^{13}C NMR (101 MHz, $CDCl_3$) δ ppm: 199.3 (C═O), 173.2 (2C, C═OO), 164.9 (olefinic−AKBA), 154.0 (Ar−OCH_3), 152.8 (Ar−OCH_3), 143.5 (CH═N), 130.6 (olefinic−AKBA), 122.0, 119.7, 112.7, 70.5, 60.6, 59.1, 56.4, 56.1, 49.0, 47.5, 45.2, 43.9, 41.0, 39.4, 39.4, 37.7, 36.7, 34.3, 34.1, 33.3, 31.0, 29.0, 27.6, 27.3, 26.7, 24.8, 21.3, 20.6, 20.0, 18.5, 17.6, 13.9; displayed a molecular ion at m/z 674.9 calculated for the molecular formula anal. calcd for $C_{41}H_{58}N_2O_6$: C, 72.96; H, 8.66; N, 4.15; found C, 72.52; H, 8.22; N, 4.30.

*4.1.9.3. E-3-Acetoxy-11-oxo-12-ursen-24-oic Acid-3,4-Dimetohxy Benzylidene Hydrazide (**16c**).* Yield 55%, mp = 200−202 °C ^{1}H NMR (400 MHz, $CDCl_3$) δ ppm: 8.5 (d, J = 5.4 Hz, 1H, NH−N═C), 8.1 (s, 1H, 1H, CH═N of a hydrazone linker), 7.4 (d, J = 1.9 Hz, 1H, Ar−H), 7.0 (dd, J = 8.3, 1.9 Hz, 1H, Ar−H), 6.8 (d, J = 8.3 Hz, 1H, Ar−H), 5.5 (s, 1H, olefinic−AKBA), 4.2 (t, J = 2.9 Hz, 1H, CH−O−AKBA), 3.9 (s, 3H−OCH_3), 3.8 (s, 3H−OCH_3), 2.5−2.4 (m, 3H), 2.1−2.0 (m, 2H), 1.8 (tdd, J = 19.9, 12.4, 4.7 Hz, 5H), 1.5−1.4 (m, 5H), 1.3 (s, 5H), 1.3 (s, 5H), 1.2−1.1 (m, 8H), 1.0−0.9 (m, 1H), 0.9 (s, 5H), 0.8−0.7 (m, 6H); ^{13}C NMR (101 MHz, $CDCl_3$) δ ppm: 199.1, (C═O)173.1 (2C, C═OO), 164.9 (olefinic−AKBA), 151.3 (Ar−OCH_3), 149.4 (Ar−OCH_3), 148 (CH═N), 130.5 (olefinic−AKBA), 126.7, 122.7, 110.5, 108.3, 70.4, 60.4, 59.0, 56.1, 55.9, 48.9, 47.4, 45.0, 43.8, 40.9, 39.3, 39.3, 37.6, 34.2, 34.0, 33.2, 30.9, 28.9, 27.5, 27.2, 26.6, 24.8, 21.1, 20.5, 19.9, 18.4, 17.4, 13.8; displayed a molecular ion at m/z 674.9 calculated for the molecular formula anal. calcd for $C_{41}H_{58}N_2O_6$: C, 72.96; H, 8.66; N, 4.15; found C, 72.78; H, 9.10; N, 3.75.

*4.1.9.4. E-3-Acetoxy-11-oxo-12-ursen-24-oic Acid-3,4,5-Trimethoxy Benzylidene Hydrazide (**16d**).* Yield 25%, mp ≥ 300 °C, ^{1}H NMR (400 MHz, $CDCl_3$) δ ppm: 8.6 (s, 1H, NH═N of a hydrazone linker), 8.3 (s, 1H, CH═N of a hydrazone linker), 7.0 (s, 2H, Ar−H), 5.6 (s, 1H, olefinic−AKBA), 4.3 (s, 1H, CH−O−AKBA), 4.0−3.9 (m, 9H−OCH_3), 2.6−2.4 (m, 3H), 2.1 (tt, J = 9.9, 4.8 Hz, 2H), 2.0−1.7 (m, 6H), 1.5 (dt, J = 13.7, 8.0 Hz, 2H), 1.4 (d, J = 19.0 Hz, 11H), 1.3−1.1 (m, 10H), 1.0 (s, 5H), 0.9−0.8 (m, 6H); ^{13}C NMR (101 MHz, $CDCl_3$) δ ppm: 199.1 (C═O), 176.3 (COO−AKBA), 173.2 (COO−AKBA), 164.8 (olefinic−AKBA), 153.7 (2C, Ar−OCH_3), 153.5 (Ar−OCH_3), 140.1 (CH═N), 130.5 (olefinic−AKBA), 129.2, 106.7, 104.7, 70.5, 61.0, 60.4, 59.0, 58.5, 56.3, 48.9, 47.5, 45.0, 43.8, 40.9, 39.3, 39.3, 37.6, 34.2, 34.0, 33.2, 30.9, 28.9, 27.5, 27.2, 26.6, 24.8, 21.1, 20.5, 20.0, 18.5, 18.4, 17.4, 13.8; displayed a molecular ion at m/z 704.95 calculated for the molecular formula anal. calcd for $C_{42}H_{60}N_2O_7$: C, 71.56; H, 8.58; N, 3.97; found C, 71.17; H, 8.16; N, 3.72.

*4.1.9.5. E-3-Acetoxy-11-oxo-12-ursen-24-oic Acid-3-Methoxy Benzylidene Hydrazide (**16e**).* Yield 50%, mp = 185−190 °C, ^{1}H NMR (400 MHz, $CDCl_3$) δ ppm: 8.6 (s, 1H, NH═N of a hydrazone linker), 8.2 (s, 1H, CH═N of a hydrazone linker), 7.3−7.1 (m, 3H, Ar−H), 6.9 (dd, J = 8.1, 2.5 Hz, 1H, Ar−H), 5.5 (s, 1H, olefinic−AKBA), 4.2 (s, 1H, CH−O−AKBA), 3.8 (s, 3H−OCH_3), 2.4 (s, 1H), 2.1−2.0 (m, 2H), 1.8 (ddd, J = 31.5, 13.2, 7.6 Hz, 6H), 1.6−1.4 (m, 6H), 1.3 (s, 5H), 1.2 (d, J = 31.1 Hz, 6H), 1.1 (d, J = 6.9 Hz, 7H), 0.9 (s, 6H), 0.8−0.7 (m, 6H);^{13}C NMR (101 MHz, $CDCl_3$) δ ppm: 199.2 (C═O), 173.4 (2C, COO−AKBA), 165.0 (olefinic−AKBA), 160.0 (Ar−OCH_3), 148.0 (CH═N), 135.2 (Ar), 130.6 (olefinic−AKBA), 129.7, 121.1, 117.5, 111.0, 70.5, 60.6, 59.1, 55.6, 49.0, 47.6, 45.2, 44.0, 41.0, 39.4, 39.4, 37.7, 34.3, 34.1, 33.3, 31.0, 29.0, 27.6, 27.3, 26.7, 24.8, 21.3, 20.6, 20.1, 18.5, 17.6, 13.9; displayed a molecular ion at m/z 644.9 calculated for the molecular formula anal. calcd for $C_{40}H_{56}N_2O_5$: 75.50; H, 8.75; N, 4.34; found C, 75.70; H, 8.99; N, 4.72.

*4.1.9.6. E-3-Acetoxy-11-oxo-12-ursen-24-oic Acid-2-Hydroxy Benzylidene Hydrazide (**16f**).* Yield 35%, mp = 271−273 °C, ^{1}H NMR (400 MHz, $CDCl_3$) δ ppm: 9.8 (brs, 1H, OH), 8.6 (s, 1H, NH═N of a hydrazone linker), 8.4 (s, 1H, CH═N of a hydrazone linker), 7.2 (d, J = 7.6 Hz, 1H, Ar−H), 7.1 (d, J = 7.5 Hz, 1H, Ar−H), 6.9 (dd, J = 8.5, 4.1 Hz, 1H, Ar−H), 6.8 (t, J = 7.4 Hz, 1H, Ar−H), 5.5 (s, 1H, olefinic−AKBA), 4.1 (s, 1H, CH−O−AKBA), 2.4 (q, J = 18.7, 16.0 Hz, 3H), 2.1−2.0 (m, 1H), 1.8 (ddd, J = 31.7, 18.9, 11.2 Hz, 4H), 1.5 (dt, J = 22.9, 10.6 Hz, 2H), 1.4−1.3 (m, 13H), 1.3 (s, 3H), 1.2 (d, J = 30.8 Hz, 4H), 1.1 (s, 2H), 1.1 (s, 2H), 1.0−0.9 (m, 1H), 0.9 (s, 4H), 0.7 (d, J = 12.6 Hz, 6H); ^{13}C NMR (101 MHz, $CDCl_3$) δ ppm: 199.1 (C═O), 172.9 (2C, COO−AKBA), 165.0 (olefinic−AKBA), 158.5 (Ar−OH), 150.9 (CH═N), 131.8 (Ar), 130.9 (Ar), 130.5 (olefinic−AKBA), 119.3, 117.5, 117.2, 70.3, 60.4, 59.0, 48.9, 47.5, 45.1, 43.9, 40.9, 39.3, 39.3, 37.5, 34.2, 34.0, 33.2, 30.9, 28.9, 27.5, 27.2, 26.6, 24.6, 21.1, 20.5, 19.9, 18.4, 17.4, 13.8; displayed a molecular ion at m/z 630.9 calculated for the molecular formula anal. calcd for $C_{39}H_{54}N_6O_4$: C, 74.25; H, 8.63; N, 4.44; found C, 73.72; H, 8.22; N, 4.1.

*4.1.9.7. E-3-Acetoxy-11-oxo-12-ursen-24-oic Acid-Piperonylidene Hydrazide (**16g**).* Yield 23%, mp ≥ 300 °C, ^{1}H NMR (400 MHz, $CDCl_3$) δ ppm: 8.5 (s, 1H, NH═N of a hydrazone linker), 8.1 (s, 1H, CH═N of a hydrazone linker), 7.3 (d, J = 1.6 Hz, 1H, Ar−H), 7.0 (dd, J = 8.0, 1.7 Hz, 1H, Ar−H), 6.7 (d, J = 8.0 Hz, 1H, Ar−H), 5.9 (s, 2H, O−CH_2−O), 5.5 (s, 1H, olefinic−AKBA), 4.2 (d, J = 2.9 Hz, 1H, CH−O−AKBA), 2.5−2.3 (m, 3H), 2.1−2.0 (m, 1H), 1.9−1.7 (m, 6H), 1.6−1.4 (m, 6H), 1.3 (s, 5H), 1.3 (s, 5H), 1.2−1.1 (m, 1H), 1.1 (d, J = 9.3 Hz, 6H), 1.0−0.9 (m, 1H), 0.9 (s, 5H), 0.8−0.7 (m, 6H); ^{13}C NMR (101 MHz, $CDCl_3$) δ ppm: 199.2 (C ═ O), 173.1 (2C, COO−AKBA), 164.9 (olefinic−AKBA), 149.7 (Ar), 148.3 (Ar), 147.6 (CH═N), 130.5, 128.2, 123.8, 108.2, 106.2, 101.5 (O−CH_2−O), 70.4, 60.5, 59.0, 48.9, 47.4, 45.1, 43.8, 40.9, 39.3, 39.3, 37.6, 34.2, 34.0, 33.2, 30.9, 28.9, 27.5, 27.2, 26.6, 24.7, 21.1, 20.5, 19.9, 18.4, 17.5, 13.8; displayed a molecular ion at m/z 658.88 calculated for the molecular formula anal. calcd for $C_{40}H_{54}N_2O_6$: C, 72.92; H, 8.26; N, 4.25; found C, 72.54; H, 8.01; N, 3.85.

*4.1.9.8. E-3-Acetoxy-11-oxo-12-ursen-24-oic Acid-3-Hydroxy-4-methoxy Benzylidene Hydrazide (**16h**).* Yield 27%, mp ≥ 300 °C, ^{1}H NMR (400 MHz, $CDCl_3$) δ ppm: 9.7 (brs, 1H, OH), 8.9 (s, 1H, NH═N of a hydrazone linker), 8.0 (s, 1H, CH═N of a hydrazone linker), 7.3 (d, J = 2.0 Hz, 1H, Ar−H), 7.0 (dd, J = 8.4, 2.0 Hz, 1H, Ar−H), 6.7 (d, J = 8.4 Hz, 1H, Ar−H), 5.5 (s, 1H, olefinic−AKBA), 4.2 (s, 1H, CH−O−AKBA), 3.8 (s, 3H−OCH_3), 2.4 (q, J = 22.3, 17.8 Hz, 5H), 2.1−2.0 (m, 1H), 1.7−1.3 (m, 9H), 1.3 (s, 4H), 1.3−1.1 (m, 7H), 1.1 (s, 7H), 1.0−0.9 (m, 1H), 0.9 (s, 5H), 0.8−0.7 (m, 6H); ^{13}C NMR (101 MHz, $CDCl_3$) δ ppm: 199.5 (C═O), 173.5 (2C, COO−AKBA), 165.1 (olefinic−AKBA), 149.1 (Ar−OCH_3), 147.9 (Ar−OH), 146.1 (CH═N), 130.5 (olefinic−AKBA), 127.0, 121.1, 112.9, 110.6, 70.3, 60.5,

https://doi.org/10.1021/acsomega.3c05247
ACS Omega 2023, 8, 39490−39510

59.0, 55.9, 49.0, 47.4, 45.1, 43.8, 40.9, 39.3, 39.3, 37.5, 34.2, 34.0, 33.2, 30.9, 28.9, 27.5, 27.2, 26.6, 24.6, 21.2, 20.5, 19.8, 18.3, 17.4, 13.9; displayed a molecular ion at m/z 660.9 calculated for the molecular formula anal. calcd for $C_{40}H_{56}N_2O_6$: C, 72.70; H, 8.54; N, 4.24; found C, 73.02; H, 8.28; N, 3.97.

*4.1.9.9. E-3-Acetoxy-11-oxo-12-ursen-24-oic Acid-4-Methoxy Benzylidene Hydrazide (**16i**).* Yield 35%, mp = 290−293 °C, ^{1}H NMR (400 MHz, $CDCl_3$) δ ppm: 8.5 (s, 1H, NH═N of a hydrazone linker), 8.1 (s, 1H, CH═N of a hydrazone linker), 7.6 (d, J = 8.3 Hz, 2H, Ar−H), 6.8 (d, J = 8.3 Hz, 2H, Ar−H), 5.5 (s, 1H, olefinic−AKBA), 4.2 (s, 1H, CH−O−AKBA), 3.8 (s, 3H, OCH_3), 2.5−2.3 (m, 3H), 2.0 (ddd, J = 16.9, 11.0, 4.2 Hz, 2H), 1.9−1.7 (m, 6H), 1.6−1.4 (m, 5H), 1.4 (d, J = 19.0 Hz, 1H), 1.3 (s, 4H), 1.3 (s, 4H), 1.2−1.2 (m, 3H), 1.1 (d, J = 7.1 Hz, 6H), 1.0−0.9 (m, 1H), 0.9 (s, 5H), 0.8−0.7 (m, 6H); ^{13}C NMR (101 MHz, $CDCl_3$) δ ppm: 199.1 (C═O), 173.1 (2C, COO−AKBA), 164.8 (olefinic−AKBA), 161.5 (Ar−OCH_3), 147.7 (CH═N), 132.0 (Ar), 130.6 (olefinic−AKBA), 129.3, 126.3, 114.3, 114.2, 70.5, 60.5, 59.0, 55.6, 55.4, 48.9, 47.4, 45.1, 43.8, 40.9, 39.3, 39.3, 37.6, 34.2, 34.0, 33.2, 30.9, 28.9, 27.5, 27.2, 26.6, 24.7, 21.2, 20.5, 19.9, 18.4, 17.5, 13.8; displayed a molecular ion at m/z 644.9 calculated for the molecular formula anal. calcd for $C_{40}H_{56}N_2O_5$: C, 74.50; H, 8.75; N, 4.34; found C, 74.80; H, 8.44; N, 4.73.

*2.1.9.10. E-3-Acetoxy-11-oxo-12-ursen-24-oic Acid-2-Cinnamylidene Hydrazide (**16j**).* Yield 30%, mp = 204−206 °C, ^{1}H NMR (400 MHz, $CDCl_3$) δ ppm: 8.7 (s, 1H, NH═N of a hydrazone linker), 8.0 (d, J = 8.8 Hz, 1H, CH═N of a hydrazone linker), 7.5−7.3 (m, 2H, Ar−H), 7.3 (t, J = 7.0 Hz, 2H, Ar−H), 7.3−7.2 (m, 1H, Ar−H), 7.0 (dd, J = 16.1, 8.7 Hz, 1H, olefinic−cinnamaldehyde), 6.8 (d, J = 15.9 Hz, 1H, olefinic−cinnamaldehyde), 5.5 (s, 1H, olefinic−AKBA), 4.2 (s, 1H, CH−O−AKBA), 2.4 (q, J = 18.0, 16.4 Hz, 3H), 2.1−2.0 (m, 3H), 1.9−1.6 (m, 5H), 1.6−1.4 (m, 5H), 1.3−1.2 (m, 9H), 1.2−1.1 (m, 1H), 1.1−1.1 (m, 6H), 1.0−0.9 (m, 1H), 0.9 (s, 5H), 0.8−0.7 (m, 7H); ^{13}C NMR (101 MHz, $CDCl_3$) δ ppm: 199.1 (C═O), 173.2 (2C, COO−AKBA), 164.9 (olefinic−AKBA), 149.4 (CH═N), 135.7 (olefinic−cinnamaldehyde), 131.3 (olefinic−cinnamaldehyde), 129.3, 129.1, 128.9, 128.5, 127.2, 124.8 (olefinic−cinnamaldehyde), 70.4, 60.4, 59.0, 48.9, 47.3, 45.0, 43.8, 40.9, 39.3, 39.3, 37.6, 34.2, 34.0, 33.2, 30.9, 28.9, 27.5, 27.2, 26.6, 24.5, 21.1, 20.5, 19.9, 18.4, 17.5, 13.7; displayed a molecular ion at m/z 640.91 calculated for the molecular formula anal. calcd for $C_{41}H_{56}N_2O_4$: C, 76.84; H, 8.81; N, 4.37; found C, 76.65; H, 9.17; N, 4.80.

*4.1.9.11. E-3-Acetoxy-11-oxo-12-ursen-24-oic Acid-2-Oxoindolin-3-ylidenehydrazide (**18**).* Yellow powder, (yield 40%), mp ≥ 300 °C, ^{1}H NMR (400 MHz, $CDCl_3$) δ ppm: 13.2 (s, 1H, NH−isatin), 7.9−7.8 (m, 2H, Ar−H, H═N of a hydrazone linker), 7.4−7.3 (m, 1H, Ar−H), 7.1 (t, J = 7.6 Hz, 1H, Ar−H), 6.9 (d, J = 7.8 Hz, 1H, Ar−H), 5.6 (s, 1H, olefinic−AKBA), 4.3 (s, 1H, CH−O−AKBA), 2.6 (d, J = 11.8 Hz, 2H), 2.5 (s, 1H), 1.9 (d, J = 9.5 Hz, 2H), 1.6 (s, 11H), 1.4 (s, 5H), 1.4 (s, 4H), 1.3 (s, 2H), 1.2 (d, J = 11.2 Hz, 7H), 1.0 (s, 5H), 0.8 (d, J = 6.2 Hz, 6H); ^{13}C NMR (101 MHz, $CDCl_3$) δ ppm: 199.3 (C═O), 174.6 (2C, COO−AKBA), 165.0 (C═O−isatin), 162.6 (olefinic−AKBA), 140.3 (C═C−NH−isatin), 136.2 (C═N−NH), 131.4 (Ar), 130.5 (olefinic−AKBA), 123.6 (Ar), 122.3 (Ar), 120.6 (Ar), 110.6 (Ar), 70.5, 60.5, 59.0, 48.9, 48.2, 45.1, 43.8, 40.9, 39.3, 37.6, 34.1, 34.0, 33.1, 30.9, 28.9, 27.5, 27.1, 26.6, 24.6, 21.1, 20.5, 19.4, 18.3, 17.5, 13.8; displayed a molecular ion at m/z 655.88 calculated for the molecular formula anal. calcd for $C_{40}H_{53}N_3O_5$: C, 73.25; H, 8.15; N, 6.41; found C, 72.84; H, 8.22; N, 6.12.

4.2. Biological Evaluation. *4.2.1. Cell Culture.* HepG2 and RAW 264.7 cell lines were obtained from VACSERA, located in Egypt. The growth of the cells was maintained at 37 °C and 5% CO_2 and in DMEM containing 10% fetal bovine serum and 1% pen−strep antibiotics until reaching 80% confluence. Cells were grown in 96-well plates in the case of cytotoxicity studies. For real-time PCR and cytokine quantification, cells were grown in six-well plates. MTT assay was used to assess the cytotoxic effect after treatment with 25 μM compounds for 24 h.

4.2.1.1. Estimation of Inflammatory Mediators in the RAW 264.7 Cell Line. The six-well plate containing the cells at a concentration of 1 × 10^6 cells/mL was treated with the hybrids at 10 and 1 μM to avoid any potential cytotoxicity or at a dose of 250 μM in the case of L-NAME. After 1 h, cells were challenged with 1 μg/mL lipopolysaccharide (Sigma-Aldrich) and incubated for 24 h. Nitric oxide levels in the supernatant collected from the cells were estimated using the Griess reagent (Biovision) according to the manufacturer's instructions. Absorbance was recorded at 540 nm. The concentration of nitrite in the media was obtained using a standard calibration curve that was assessed simultaneously with the samples.

4.2.1.2. qPCR Analysis. Based on the ability of the compounds to achieve better activity than L-NAME, eight compounds were selected for qPCR study to determine their ability to reduce the gene expression of TNF-α at 10 μM in comparison to dexamethasone as a standard at a dose of 1 μM. The pelleted cells were subjected to RNA extraction using a TRIzol reagent according to the manufacturer's protocol and stored at −80 °C for real-time PCR. Thus, cDNA was synthesized from total RNA using a cDNA reverse transcription kit (Thermoscientific), and mRNA expression was subsequently amplified using a SYBR Green qPCR Master Mix following the manufacturer's protocol (Thermoscientific). Gene-specific primers shown in Table S25 were mixed with synthesized cDNA and SYBR Green qPCR Master according to the manufacturer's instructions and subjected to amplification using a Step One real-time thermal cycler applying the following settings: incubation at 94 °C for 15 s, annealing at 60 °C for 30 s, and extension at 72 °C for 30 s. To determine the fold change in gene expression levels of the target genes, the data were normalized to the GAPDH values using the $2^{-\Delta\Delta Ct}$ comparative cycle threshold method.

4.2.1.3. Evaluation of Anti-inflammatory and Hepatoprotective Effects of the Compounds against APAP Hepatotoxicity in HepG2. Based on qPCR analysis, compounds **5b** and **18** have been chosen for further investigation by determining their ability to mitigate APAP hepatotoxicity. Therefore, HepG2 cells were grown at 1 × 10^6 confluence and were divided into cells treated with vehicle (DMSO) only, cells that received treatment with 1 and 10 μM tested compounds or 25 μg/mL silymarin as a positive control hepatoprotective agent,[80] and cells induced by APAP only (toxicity model). After 24 h, 10 mM APAP was added to all cells except the control to induce hepatotoxicity for another 24 h. ELISA kits (FineTest, China) were used to estimate levels of cytokines such as tumor necrosis factor-α (TNF-α), interleukin-1β (IL-1β), and interleukin-6 (IL-6) using the cell supernatant

https://doi.org/10.1021/acsomega.3c05247
ACS Omega 2023, 8, 39490−39510

centrifuged at 4 °C at 1000xg for 20 min. Total protein concentration was determined by Lowry's method, and commercial assay kits (Biodiagnostic, Egypt) were used to determine the level of oxidative stress markers such as GSH,[81] MDA,[82] and SOD,[83] as instructed by the manufacturer.

4.3. Statistical Analysis. GraphPad prism V 8.0 was used for group comparison. Data were shown as mean ± SEM, and one-way analysis of variance (one-way ANOVA) was selected for statistical analysis. A p-value of ≤0.05 was considered statistically significant.

4.4. *In Silico* Identification of the Mechanism of Action of the AKBA Hybrid. *4.4.1. Network Pharmacology.* The PharmMapper server (http://www.lilab-ecust.cn/pharmmapper/)[84] and the Swiss target prediction server[85] were used to determine the potential target of compounds **5b** and **18**. Duplicates were excluded from the combined targets, and the resulting list was saved as a CSV file. Also, the molecular target list linked to hepatitis, hepatotoxicity, and liver injury was gathered from the Input 2.0 server.[86] Afterward, common targets were identified by comparing the two lists by the Venny 2.1.0 tool (https://bioinfogp.cnb.csic.es/tools/venny/).

The identified common targets were subjected to enrichment analysis where gene ontology was conducted and the most relevant biological processes (BP), molecular functions (MF), and cellular components (CC) were identified; also, the analysis of the Kyoto Encyclopedia of Genes and Genomes (KEGG) pathways was done. Finally, a protein−protein interaction network was generated based on confidence score = 0.7. Then, gene distribution analysis was utilized to highlight targets that are significantly correlated to the activity of the compounds

4.4.2. Molecular Docking. PI3K was found as the most significant target for compounds **5b** and **18** based on system pharmacology analysis. So, their binding mode was investigated using molecular docking. In summary, the PDB files of (PI3K): **3HHM** and compounds **5b** and **18**'s 3D chemical structures were submitted to protein and ligand optimization panels integrated in the CB-Dock2 online server, respectively. The blind docking approach was utilized to study the interaction of the compounds with identified active sites. After that, poses are ranked according to their score.[87] Finally, the best pose was visualized to study its interaction with the binding site through the Discovery studio visualizer.[88]

4.4.3. ADMET Prediction. To gain insights into the pharmacokinetic properties of the most active hybrids, the chemical structures of compounds **5b** and **18** as submitted to ADMET prediction server PkCSM (https://biosig.lab.uq.edu.au/pkcsm/), which uses graph-based signature for the assessment of pharmacokinetic properties of the compound.[89] Also, the PreADMET server[90] was used (https://preadmet.webservice.bmdrc.org/) to compare the results and ensure its reproducibility. Predicted LD_{50} is calculated using the ProTox-II server (https://tox-new.charite.de/protox_II/index.php?site=home), which uses molecular similarity, fragment propensities, and machine learning to identify the potential toxicity of compounds.[91]

4.5. Chemical Stability Studies. *4.5.1. HPLC Analysis.* All chromatographic separations were conducted using the Dionex UltiMate 3000RS HPLC system. Samples (20 μL) were injected into an Inertsil C18 column (150 × 4.6 mm × 5 μm.). HPLC conditions were conducted as previously reported,[32] using a mixture of acetonitrile and water in a ratio of 90:10 (v/v %) as a mobile phase, and glacial acetic acid was used to adjust pH to 4. A flow rate of 1.2 mL/min was used during all of the runs. The calibration curve of compounds was constructed by plotting their peak areas against a series of known concentrations of 12.5 to 150 μM.

4.5.2. In Vitro Hydrolysis. The hydrolysis of the conjugates was studied using buffer solutions at pH 1.2 and pH 7.4 to mimic gastric and intestinal environment, respectively. Compounds **5b** and **18** (75 μM) were placed in capped 50 mL Erlenmeyer flasks containing 50 mL of either 0.1 M HCl (pH 1.4) or phosphate buffer (pH 7.4) and kept at a constant temperature of 37 °C. Samples were taken at certain time intervals (0, 60, 120, 180, 240 min), and their % concentration was quantified using HPLC analysis. Based on the hydrolysis of the compounds, reaction rate constants (Kobs) and their half-life ($t_{1/2}$) values were then calculated.[92]

■ ASSOCIATED CONTENT

Supporting Information

The Supporting Information is available free of charge at https://pubs.acs.org/doi/10.1021/acsomega.3c05247.

^{1}H NMR and ^{13}C NMR spectra of all compounds (Figure S1−S46), their full assignments (Table S1−S23), targets identified by network pharmacology (Table S24), and primers used in real-time PCR study (Table S25) (PDF)

■ AUTHOR INFORMATION

Corresponding Author

Farid A. Badria − *Department of Pharmacognosy, Faculty of Pharmacy, Mansoura University, Mansoura 35516, Egypt;* orcid.org/0000-0001-8596-5589; Phone: +20) 1001762927; Email: faridbadria@gmail.com

Authors

Abdullah A. Elgazar − *Department of Pharmacognosy, Faculty of Pharmacy, Kafrelsheikh University, Kafrelsheikh 33516, Egypt;* orcid.org/0000-0002-5851-3306

Ramadan A. El-Domany − *Department of Microbiology and Immunology, Faculty of Pharmacy, Kafrelsheikh University, Kafrelsheikh 33516, Egypt*

Wagdy M. Eldehna − *Department of Pharmaceutical Chemistry, Faculty of Pharmacy, Kafrelsheikh University, Kafrelsheikh 33516, Egypt;* orcid.org/0000-0001-6996-4017

Complete contact information is available at: https://pubs.acs.org/10.1021/acsomega.3c05247

Notes

The authors declare no competing financial interest.

■ ACKNOWLEDGMENTS

The authors have nothing to disclose, and this research received no specific grant from any funding resources.

■ REFERENCES

(1) Peters, J.-U. Polypharmacology − Foe or Friend. *J. Med. Chem.* **2013**, *56* (22), 8955−8971.

(2) Pelkonen, O.; Xu, Q.; Fan, T.-P. Why is Research on Herbal Medicinal Products Important and How Can We Improve Its Quality? *J. Tradit. Complementary Med.* **2014**, *4* (1), 1−7.

(3) Jansen, C.; Baker, J. D.; Kodaira, E.; Ang, L.; Bacani, A. J.; Aldan, J. T.; Shimoda, L. M. N.; Salameh, M.; Small-Howard, A. L.; Stokes,

A. J.; et al. Medicine in motion: Opportunities, challenges and data analytics-based solutions for traditional medicine integration into western medical practice. *J. Ethnopharmacol.* **2021**, *267*, No. 113477.
(4) Li, P.; Chen, J.; Zhang, W.; Fu, B.; Wang, W. Transcriptome inference and systems approaches to polypharmacology and drug discovery in herbal medicine. *J. Ethnopharmacol.* **2017**, *195*, 127−136.
(5) Hodon, J.; Borkova, L.; Pokorny, J.; Kazakova, A.; Urban, M. Design and synthesis of pentacyclic triterpene conjugates and their use in medicinal research. *Eur. J. Med. Chem.* **2019**, *182*, No. 111653.
(6) Suneela, D.; Dipmala, P. Synthesis and pharmacokinetic profile of rhein- boswellic acid conjugate. *Bioorg. Med. Chem. Lett.* **2012**, *22* (24), 7582−7587.
(7) Shenvi, S.; Kiran, K. R.; Kumar, K.; Diwakar, L.; Reddy, G. C. Synthesis and biological evaluation of boswellic acid-NSAID hybrid molecules as anti-inflammatory and anti-arthritic agents. *Eur. J. Med. Chem.* **2015**, *98*, 170−178.
(8) Huang, M.; Li, A.; Zhao, F.; Xie, X.; Li, K.; Jing, Y.; Liu, D.; Zhao, L. Design, synthesis and biological evaluation of ring A modified 11-keto-boswellic acid derivatives as Pin1 inhibitors with remarkable anti-prostate cancer activity. *Bioorg. Med. Chem. Lett.* **2018**, *28* (19), 3187−3193.
(9) Rehman, N. U.; Ullah, S.; Alam, T.; Halim, S. A.; Mohanta, T. K.; Khan, A.; Anwar, M. U.; Csuk, R.; Avula, S. K.; Al-Harrasi, A. Discovery of New Boswellic Acid Hybrid 1H-1,2,3-Triazoles for Diabetic Management: In Vitro and In Silico Studies. *Pharmaceuticals* **2023**, *16*, No. 229, DOI: 10.3390/ph16020229.
(10) Asad, M.; Alhumoud, M. Hepatoprotective effect and GC-MS analysis of traditionally used Boswellia sacra oleo gum resin (Frankincense) extract in. *Afr. J. Tradit., Complementary Altern. Med.* **2015**, *12* (2), 1−5.
(11) Marefati, N.; Beheshti, F.; Etemadizadeh, P.; Hosseini, M.; Anaeigoudari, A. Gum resin extract of Boswellia serrata attenuates lipopolysaccharide-induced inflammation and oxidative damage in hepatic and renal tissues of rats. *Asian Pac. J. Trop. Biomed.* **2022**, *12* (1), 20−25.
(12) Jyothi, Y.; Kamath, J. V.; Asad, M. Effect of hexane extract of Boswellia serrata oleo-gum resin on chemically induced liver damage. *Pak J. Pharm. Sci.* **2006**, *19* (2), 125−129.
(13) Houssen, M. E.; Ragab, A.; Mesbah, A.; El-Samanoudy, A. Z.; Othman, G.; F Moustafa, A.; Badria, F. A. Natural anti-inflammatory products and leukotriene inhibitors as complementary therapy for bronchial asthma. *Clin. Biochem.* **2010**, *43* (10), 887−890.
(14) Farid, A. B. Frankincense (Heaven's Gift) — Chemistry, Biology, and Clinical Applications. In *Evidence-based Strategies in Herbal Medicine, Psychiatric Disorders and Emergency Medicine*; Farid, A. B., Ed.; IntechOpen, 2015; Chapter 1.
(15) Kumar, M.; Singh, G.; Bhardwaj, P.; Dhatwalia, S. K.; Dhawan, D. K. Understanding the role of 3-O-Acetyl-11-keto-β-boswellic acid in conditions of oxidative-stress mediated hepatic dysfunction during benzo(a)pyrene induced toxicity. *Food Chem. Toxicol.* **2017**, *109*, 871−878.
(16) Eltahir, H. M.; Fawzy, M. A.; Mohamed, E. M.; Alrehany, M. A.; Shehata, A. M.; Abouzied, M. M. Antioxidant, anti-inflammatory and anti-fibrotic effects of Boswellia serrate gum resin in CCl4-induced hepatotoxicity. *Exp. Ther. Med.* **2019**, *19* (2), 1313−1321.
(17) Choudhary, S.; Singh, P. K.; Verma, H.; Singh, H.; Silakari, O. Success stories of natural product-based hybrid molecules for multi-factorial diseases. *Eur. J. Med. Chem.* **2018**, *151*, 62−97.
(18) Bhushan, B.; Apte, U. Liver Regeneration after Acetaminophen Hepatotoxicity: Mechanisms and Therapeutic Opportunities. *Am. J. Pathol.* **2019**, *189* (4), 719−729.
(19) Chilvery, S.; Yelne, A.; Khurana, A.; Saifi, M. A.; Bansod, S.; Anchi, P.; Godugu, C. Acetaminophen induced hepatotoxicity: An overview of the promising protective effects of natural products and herbal formulations. *Phytomedicine* **2023**, *108*, No. 154510.
(20) ElGamal, R. A.; Galala, A. A.; Abdel-Kader, M. S.; Badria, F. A.; Soliman, A. F. Microbial Transformation of the Sesquiterpene Lactone, Vulgarin, by Aspergillus niger. *Molecules* **2023**, *28* (9), 3729.
(21) Omar, R. M.; Badria, F. A.; Galala, A. A. An emerging flavone glycoside from Phyllanthus emblica L.: A promiscuous enzyme inhibitor and potential therapeutic in chronic diseases. *S. Afr. J. Bot.* **2023**, *153*, 290−296.
(22) Elimam, D. M.; Elgazar, A. A.; Bonardi, A.; Abdelfadil, M.; Nocentini, A.; El-Domany, R. A.; Abdel-Aziz, H. A.; Badria, F. A.; Supuran, C. T.; Eldehna, W. M. Natural inspired piperine-based sulfonamides and carboxylic acids as carbonic anhydrase inhibitors: Design, synthesis and biological evaluation. *Eur. J. Med. Chem.* **2021**, *225*, No. 113800.
(23) Elattar, E. M.; Galala, A. A.; Saad, H.-E. A.; Badria, F. A. Hyaluronidase Inhibitory Activity and In Silico Docking Study of New Eugenol 1,2,3-triazole Derivatives. *ChemistrySelect* **2022**, *7* (42), No. e202202194.
(24) El-Naggar, M. H.; Abdel Bar, F. M.; Harsha, C.; Monisha, J.; Shimizu, K.; Kunnumakkara, A. B.; Badria, F. A. Synthesis of new selective cytotoxic ricinine analogues against oral squamous cell carcinoma. *Nat. Prod. Res.* **2021**, *35* (13), 2145−2156.
(25) El-Naggar, M. H.; Mira, A.; Abdel Bar, F. M.; Shimizu, K.; Amer, M. M.; Badria, F. A. Synthesis, docking, cytotoxicity, and LTA4H inhibitory activity of new gingerol derivatives as potential colorectal cancer therapy. *Bioorg. Med. Chem.* **2017**, *25* (3), 1277−1285.
(26) Abdel Bar, F. M.; Elimam, D. M.; Mira, A. S.; El-Senduny, F. F.; Badria, F. A. Derivatization, molecular docking and in vitro acetylcholinesterase inhibitory activity of glycyrrhizin as a selective anti-Alzheimer agent. *Nat. Prod. Res.* **2019**, *33* (18), 2591−2599.
(27) Elgazar, A. A.; El-Domany, R. A.; Eldehna, W. M.; Badria, F. A. Theophylline-based hybrids as acetylcholinesterase inhibitors endowed with anti-inflammatory activity: synthesis, bioevaluation, in silico and preliminary kinetic studies. *RSC Adv.* **2023**, *13* (36), 25616−25634.
(28) Avula, S. K.; Rehman, N. U.; Khan, F.; Ullah, O.; Halim, S. A.; Khan, A.; Anwar, M. U.; Rahman, S. M.; Csuk, R.; Al-Harrasi, A. Triazole-tethered boswellic acid derivatives against breast cancer: Synthesis, in vitro, and in-silico studies. *J. Mol. Struct.* **2023**, *1282*, No. 135181.
(29) Chaturvedi, D.; Dwivedi, P. K.; Chaturvedi, A. K.; Mishra, N.; Siddiqui, H. H.; Mishra, V. Semisynthetic hybrids of boswellic acids: a novel class of potential anti-inflammatory and anti-arthritic agents. *Med. Chem. Res.* **2015**, *24* (7), 2799−2812.
(30) Avula, S. K.; Rehman, N. U.; Khan, M.; Halim, S. A.; Khan, A.; Rafiq, K.; Csuk, R.; Das, B.; Al-Harrasi, A. New synthetic 1H-1,2,3-triazole derivatives of 3-O-acetyl-β-boswellic acid and 3-O-acetyl-11-keto-β-boswellic acid from Boswellia sacra inhibit carbonic anhydrase II in vitro. *Med. Chem. Res.* **2021**, *30* (6), 1185−1198.
(31) Neises, B.; Steglich, W. Simple Method for the Esterification of Carboxylic Acids. *Angew. Chem., Int. Ed.* **1978**, *17* (7), 522−524.
(32) Badria, F.; Mazyed, E. Formulation of Nanospanlastics as a Promising Approach for Improving the Topical Delivery of a Natural Leukotriene Inhibitor (3-Acetyl-11-Keto-β-Boswellic Acid): Statistical Optimization, in vitro Characterization, and ex vivo Permeation Study. *Drug Des., Dev. Ther.* **2020**, *14*, 3697−3721. From NLM.
(33) Yamaji, T.; Saito, T.; Hayamizu, K.; Yanagisawa, M.; Yamamoto, O. *Spectral Database for Organic Compounds SDBS*; National Institute of Advanced Industrial Science and Technology (AIST): Japan.
(34) Sharma, H.; Kumar, P.; Deshmukh, R. R.; Bishayee, A.; Kumar, S. Pentacyclic triterpenes: New tools to fight metabolic syndrome. *Phytomedicine* **2018**, *50*, 166−177.
(35) Chen, L.-C.; Hu, L.-H.; Yin, M.-C. Alleviative effects from boswellic acid on acetaminophen-induced hepatic injury. *BioMedicine* **2016**, *6* (2), No. 9.
(36) Ammon, H. P. T. Boswellic Acids in Chronic Inflammatory Diseases. *Planta Med.* **2006**, *72* (12), 1100−1116.
(37) Martínez-Clemente, M.; Ferré, N.; González-Périz, A.; López-Parra, M.; Horrillo, R.; Titos, E.; Morán-Salvador, E.; Miquel, R.; Arroyo, V.; Funk, C. D.; Clària, J. 5-lipoxygenase deficiency reduces hepatic inflammation and tumor necrosis factor α−induced

https://doi.org/10.1021/acsomega.3c05247
ACS Omega 2023, 8, 39490−39510

hepatocyte damage in hyperlipidemia-prone ApoE-null mice. *Hepatology* **2010**, *51* (3), 817−827.
(38) Safayhi, H.; Mack, T.; Sabieraj, J.; Anazodo, M. I.; Subramanian, L. R.; Ammon, H. P. Boswellic acids: novel, specific, nonredox inhibitors of 5-lipoxygenase. *J. Pharmacol. Exp. Ther.* **1992**, *261* (3), 1143−1146.
(39) Zaitone, S. A.; Barakat, B. M.; Bilasy, S. E.; Fawzy, M. S.; Abdelaziz, E. Z.; Farag, N. E. Protective effect of boswellic acids versus pioglitazone in a rat model of diet-induced non-alcoholic fatty liver disease: influence on insulin resistance and energy expenditure. *Naunyn-Schmiedeberg's Arch. Pharmacol.* **2015**, *388* (6), 587−600.
(40) Thabet, N. M.; Abdel-Rafei, M. K.; Moustafa, E. M. Boswellic acid protects against Bisphenol-A and gamma radiation induced hepatic steatosis and cardiac remodelling in rats: role of hepatic PPAR-α/P38 and cardiac Calcineurin-A/NFATc1/P38 pathways. *Arch. Physiol. Biochem.* **2022**, *128* (3), 767−785.
(41) Barakat, B. M.; Ahmed, H. I.; Bahr, H. I.; Elbahaie, A. M. Protective Effect of Boswellic Acids against Doxorubicin-Induced Hepatotoxicity: Impact on Nrf2/HO-1 Defense Pathway. *Oxid. Med. Cell. Longevity* **2018**, *2018*, No. 8296451.
(42) Gabbai-Armelin, P. R.; Sales, L. S.; Ferrisse, T. M.; De Oliveira, A. B.; De Oliveira, J. R.; Giro, E. M. A.; Brighenti, F. L. A systematic review and meta-analysis of the effect of thymol as an anti-inflammatory and wound healing agent. *Phytother. Res.* **2022**, *36* (9), 3415−3443.
(43) Guo, C.; Zheng, L.; Chen, S.; Liang, X.; Song, X.; Wang, Y.; Hua, B.; Qiu, L. Thymol ameliorates ethanol-induced hepatotoxicity via regulating metabolism and autophagy. *Chem.-Biol. Interact.* **2023**, *370*, No. 110308.
(44) Dou, X.; Yan, D.; Liu, S.; Gao, L.; Shan, A. Thymol Alleviates LPS-Induced Liver Inflammation and Apoptosis by Inhibiting NLRP3 Inflammasome Activation and the AMPK-mTOR-Autophagy Pathway. *Nutrients* **2022**, *14* (14), 2809.
(45) Ogaly, H. A.; Abdel-Rahman, R. F.; Mohamed, M. A. E.; OA, A.-F.; Khattab, M. S.; Abd-Elsalam, R. M. Thymol ameliorated neurotoxicity and cognitive deterioration in a thioacetamide-induced hepatic encephalopathy rat model; involvement of the BDNF/CREB signaling pathway. *Food Function* **2022**, *13* (11), 6180−6194.
(46) Palabiyik, S.; Karakus, E.; Halici, Z.; Cadirci, E.; Bayir, Y.; Ayaz, G.; Cinar, I. The protective effects of carvacrol and thymol against paracetamol−induced toxicity on human hepatocellular carcinoma cell lines (HepG2). *Hum. Exp. Toxicol.* **2016**, *35* (12), 1252−1263.
(47) Gillam, E. M. J.; Notley, L. M.; Cai, H.; De Voss, J. J.; Guengerich, F. P. Oxidation of Indole by Cytochrome P450 Enzymes. *Biochemistry* **2000**, *39* (45), 13817−13824.
(48) Maugard, T.; Enaud, E.; Choisy, P.; Legoy, M. D. Identification of an indigo precursor from leaves of Isatis tinctoria (Woad). *Phytochemistry* **2001**, *58* (6), 897−904.
(49) Nagle, A. A.; Reddy, S. A.; Bertrand, H.; Tajima, H.; Dang, T.-M.; Wong, S.-C.; Hayes, J. D.; Wells, G.; Chew, E.-H. 3-(2-Oxoethylidene)indolin-2-one Derivatives Activate Nrf2 and Inhibit NF-κB: Potential Candidates for Chemoprevention. *ChemMedChem* **2014**, *9* (8), 1763−1774.
(50) Medvedev, A.; Buneeva, O.; Glover, V. Biological targets for isatin and its analogues: Implications for therapy. *Biol.: Targets Ther.* **2007**, *1* (2), 151−162.
(51) Andreani, A.; Burnelli, S.; Granaiola, M.; Leoni, A.; Locatelli, A.; Morigi, R.; Rambaldi, M.; Varoli, L.; Cremonini, M. A.; Placucci, G.; et al. New isatin derivatives with antioxidant activity. *Eur. J. Med. Chem.* **2010**, *45* (4), 1374−1378.
(52) Tejasree, C.; Kiran, G.; Rajyalakshmi, G.; Rama Narsimha Reddy, A. Hepatoprotective activity of 1-(4-(Dimethylamino)-Benzylidene)-5-(2-Oxoindolin-3-ylidene) Thiocarbohydrazone in rats. *Toxicol. Environ. Chem.* **2013**, *95* (9), 1589−1594.
(53) Tawfik, N. G.; Mohamed, W. R.; Mahmoud, H. S.; Alqarni, M. A.; Naguib, I. A.; Fahmy, A. M.; Ahmed, O. M. Isatin Counteracts Diethylnitrosamine/2-Acetylaminofluorene-Induced Hepatocarcinogenesis in Male Wistar Rats by Upregulating Anti-Inflammatory, Antioxidant, and Detoxification Pathways. *Antioxidants* **2022**, *11* (4), 699.
(54) Bhushan, B.; Michalopoulos, G. K. Role of epidermal growth factor receptor in liver injury and lipid metabolism: Emerging new roles for an old receptor. *Chem.-Biol. Interact.* **2020**, *324*, No. 109090.
(55) Wang, Y.-P.; Wang, Y.-D.; Liu, Y.-P.; Cao, J.-X.; Yang, M.-L.; Wang, Y.-F.; Khan, A.; Zhao, T.-R.; Cheng, G.-G. 6′-O-Caffeoylarbutin from Que Zui tea ameliorates acetaminophen-induced liver injury via enhancing antioxidant ability and regulating the PI3K signaling pathway. *Food Function* **2022**, *13* (9), 5299−5316.
(56) Zhao, J.-H.; Li, J.; Zhang, X.-Y.; Shi, S.; Wang, L.; Yuan, M.-L.; Liu, Y.-P.; Wang, Y.-D. Confusoside from Anneslea fragrans Alleviates Acetaminophen-Induced Liver Injury in HepG2 via PI3K-CASP3 Signaling Pathway. *Molecules* **2023**, *28* (4), 1932.
(57) Roy, N. K.; Parama, D.; Banik, K.; Bordoloi, D.; Devi, A. K.; Thakur, K. K.; Padmavathi, G.; Shakibaei, M.; Fan, L.; Sethi, G.; Kunnumakkara, A. B. An Update on Pharmacological Potential of Boswellic Acids against Chronic Diseases. *Int. J. Mol. Sci.* **2019**, *20* (17), 4101.
(58) Peron, G.; Marzaro, G.; Dall'Acqua, S. Known Triterpenes and their Derivatives as Scaffolds for the Development of New Therapeutic Agents for Cancer. *Curr. Med. Chem.* **2018**, *25* (10), 1259−1269.
(59) Hussein, R. M.; Arafa, E.-S. A.; Raheem, S. A.; Mohamed, W. R. Thymol protects against bleomycin-induced pulmonary fibrosis via abrogation of oxidative stress, inflammation, and modulation of miR-29a/TGF-β and PI3K/Akt signaling in mice. *Life Sci.* **2023**, *314*, No. 121256.
(60) Eakins, R.; Walsh, J.; Randle, L.; Jenkins, R. E.; Schuppe-Koistinen, I.; Rowe, C.; Starkey Lewis, P.; Vasieva, O.; Prats, N.; Brillant, N.; et al. Adaptation to acetaminophen exposure elicits major changes in expression and distribution of the hepatic proteome. *Sci. Rep.* **2015**, *5*, No. 16423. From NLM
(61) Salama, R. M.; Abbas, S. S.; Darwish, S. F.; Sallam, A. A.; Elmongy, N. F.; El Wakeel, S. A. Regulation of NOX/p38 MAPK/PPARα pathways and miR-155 expression by boswellic acids reduces hepatic injury in experimentally-induced alcoholic liver disease mouse model: novel mechanistic insight. *Arch. Pharmacal Res.* **2023**, *46* (4), 323−338.
(62) Bruno, M. K.; Khairallah, E. A.; Cohen, S. D. Inhibition of Protein Phosphatase Activity and Changes in Protein Phosphorylation Following Acetaminophen Exposure in Cultured Mouse Hepatocytes. *Toxicol. Appl. Pharmacol.* **1998**, *153* (1), 119−132.
(63) Poeckel, D.; Werz, O. Boswellic Acids: Biological Actions and Molecular Targets. *Curr. Med. Chem.* **2006**, *13* (28), 3359−3369.
(64) Bidula, S.; Sexton, D. W.; Schelenz, S. Ficolins and the Recognition of Pathogenic Microorganisms: An Overview of the Innate Immune Response and Contribution of Single Nucleotide Polymorphisms. *J. Immunol. Res.* **2019**, *2019*, No. 3205072.
(65) Wagner, E.; Frank, M. M. Therapeutic potential of complement modulation. *Nat. Rev. Drug Discovery* **2010**, *9* (1), 43−56.
(66) Wang, J.; Zhang, L.; Shi, Q.; Yang, B.; He, Q.; Wang, J.; Weng, Q. Targeting innate immune responses to attenuate acetaminophen-induced hepatotoxicity. *Biochem. Pharmacol.* **2022**, *202*, No. 115142.
(67) Franco-Trepat, E.; Alonso-Pérez, A.; Guillán-Fresco, M.; López-Fagúndez, M.; Pazos-Pérez, A.; Crespo-Golmar, A.; Belén Bravo, S.; López-López, V.; Jorge-Mora, A.; Cerón-Carrasco, J. P.; et al. β Boswellic Acid Blocks Articular Innate Immune Responses: An In Silico and In Vitro Approach to Traditional Medicine. *Antioxidants* **2023**, *12* (2), No. 371.
(68) Kapil, A.; Moza, N. Anticomplementary activity of Boswellic acids — An inhibitor of C3-convertase of the classical complement pathway. *Int. J. Immunopharmacol.* **1992**, *14* (7), 1139−1143.
(69) Knaus, U.; Wagner, H. Effects of boswellic acid of Boswellia serrata and other triterpenic acids on the complement system. *Phytomedicine* **1996**, *3* (1), 77−80.
(70) Wang, Q.; Zhang, P.; Zhang, W.; Zhang, X.; Chen, J.; Ding, P.; Li, L.; Lv, X.; Li, L.; Hu, W. PI3K activation is enhanced by FOXM1D

https://doi.org/10.1021/acsomega.3c05247
ACS Omega 2023, 8, 39490−39510

binding to p110 and p85 subunits. *Signal Transduction Targeted Ther.* **2020**, *5* (1), 105. From NLM
(71) Ghosh, S.; Sarkar, A.; Bhattacharyya, S.; Sil, P. C. Silymarin Protects Mouse Liver and Kidney from Thioacetamide Induced Toxicity by Scavenging Reactive Oxygen Species and Activating PI3K-Akt Pathway. *Front. Pharmacol.* **2016**, *7*, No. 481.
(72) Wang, Z.; Hao, W.; Hu, J.; Mi, X.; Han, Y.; Ren, S.; Jiang, S.; Wang, Y.; Li, X.; Li, W. Maltol Improves APAP-Induced Hepatotoxicity by Inhibiting Oxidative Stress and Inflammation Response via NF-κB and PI3K/Akt Signal Pathways. *Antioxidants* **2019**, *8* (9), No. 395, DOI: 10.3390/antiox8090395.
(73) Othman, D. I. A.; Hamdi, A.; Tawfik, S. S.; Elgazar, A. A.; Mostafa, A. S. Identification of new benzimidazole-triazole hybrids as anticancer agents: multi-target recognition, in vitro and in silico studies. *J. Enzyme Inhib. Med. Chem.* **2023**, *38* (1), No. 2166037.
(74) Al-Sanea, M. M.; Hamdi, A.; Mohamed, A. A. B.; El-Shafey, H. W.; Moustafa, M.; Elgazar, A. A.; Eldehna, W. M.; Ur Rahman, H.; Parambi, D. G. T.; Elbargisy, R. M.; et al. New benzothiazole hybrids as potential VEGFR-2 inhibitors: design, synthesis, anticancer evaluation, and in silico study. *J. Enzyme Inhib. Med. Chem.* **2023**, *38* (1), No. 2166036.
(75) Sánchez, D. A.; Tonetto, G. M.; Ferreira, M. L. Enzymatic Synthesis of Thymol Octanoate, a Promising Hybrid Molecule. *Catalysts* **2023**, *13* (3), 473.
(76) Matesic, L.; Locke, J. M.; Vine, K. L.; Ranson, M.; Bremner, J. B.; Skropeta, D. Synthesis and hydrolytic evaluation of acid-labile imine-linked cytotoxic isatin model systems. *Bioorg. Med. Chem.* **2011**, *19* (5), 1771−1778.
(77) Badria, F. A.; Mikhaeil, B. R.; Maatooq, G. T.; Amer, M. M. A. Immunomodulatory Triterpenoids from the Oleogum Resin of Boswellia carterii Birdwood. *Z. Naturforsch., C* **2003**, *58* (7−8), 505−516.
(78) Rao, M. L.; Kumar, A. J. T. Pd-catalyzed chemo-selective mono-arylations and bis-arylations of functionalized 4-chlorocoumarins with triarylbismuths as threefold arylating reagents. *Tetrahedron* **2014**, *70* (39), 6995−7005.
(79) Zhao, J.-W.; Wu, Z.-H.; Guo, J.-W.; Huang, M.-J.; You, Y.-Z.; Liu, H.-M.; Huang, L.-H. J. E. J. o. M. C. Synthesis and anti-gastric cancer activity evaluation of novel triazole nucleobase analogues containing steroidal/coumarin/quinoline moieties. *Eur. J. Med. Chem.* **2019**, *181*, No. 111520.
(80) Ali, M. Y.; Jannat, S.; Jung, H. A.; Min, B.-S.; Paudel, P.; Choi, J. S. Hepatoprotective effect of Cassia obtusifolia seed extract and constituents against oxidative damage induced by tert-butyl hydroperoxide in human hepatic HepG2 cells. *J. Food Biochem.* **2018**, *42* (1), No. e12439.
(81) Beutler, E.; Duron, O.; Kelly, B. M. Improved method for the determination of blood glutathione. *J. Lab. Clin. Med.* **1963**, *61*, 882−888. From NLM
(82) Ohkawa, H.; Ohishi, N.; Yagi, K. Assay for lipid peroxides in animal tissues by thiobarbituric acid reaction. *Anal. Biochem.* **1979**, *95* (2), 351−358.
(83) Nishikimi, M.; Appaji Rao, N.; Yagi, K. The occurrence of superoxide anion in the reaction of reduced phenazine methosulfate and molecular oxygen. *Biochem. Biophys. Res. Commun.* **1972**, *46* (2), 849−854.
(84) Wang, X.; Shen, Y.; Wang, S.; Li, S.; Zhang, W.; Liu, X.; Lai, L.; Pei, J.; Li, H. J. N. a. r. PharmMapper 2017 update: a web server for potential drug target identification with a comprehensive target pharmacophore database. *Nucleic Acids Res.* **2017**, *45* (W1), W356−W360.
(85) Gfeller, D.; Michielin, O.; Zoete, V. Shaping the interaction landscape of bioactive molecules. *Bioinformatics* **2013**, *29* (23), 3073−3079.
(86) Li, X.; Tang, Q.; Meng, F.; Du, P.; Chen, W. INPUT: An intelligent network pharmacology platform unique for traditional Chinese medicine. *Comput. Struct. Biotechnol. J.* **2022**, *20*, 1345−1351.
(87) El-Senduny, F. F.; Elgazar, A. A.; Alwasify, H. A.; Abed, A.; Foda, M.; Abouzeid, S.; Lewerenz, L.; Selmar, D.; Badria, F. Bio-evaluation of Untapped Alkaloids from Vinca minor Enriched by Methyl-jasmonate-induced Stress: an Integrated Approach. *Planta Med.* **2023**, *89*, 964−978, DOI: 10.1055/a-2058-3863.
(88) Elimam, D. M.; Elgazar, A. A.; El-Senduny, F. F.; El-Domany, R. A.; Badria, F. A.; Eldehna, W. M. Natural inspired piperine-based ureas and amides as novel antitumor agents towards breast cancer. *J. Enzyme Inhib. Med. Chem.* **2022**, *37* (1), 39−50.
(89) Pires, D. E. V.; Blundell, T. L.; Ascher, D. B. pkCSM: Predicting Small-Molecule Pharmacokinetic and Toxicity Properties Using Graph-Based Signatures. *J. Med. Chem.* **2015**, *58* (9), 4066−4072.
(90) Lee, S. K.; Lee, I. H.; Kim, H. J.; Chang, G. S.; Chung, J. E.; No, K. T. *The preADME Approach: Web-Based Program for Rapid Prediction Processes, Problems, and Solutions*; Blackwell Publishing, Malden, MA, USA, 2003.
(91) Banerjee, P.; Eckert, A. O.; Schrey, A. K.; Preissner, R. ProTox-II: a webserver for the prediction of toxicity of chemicals. *Nucleic Acids Res.* **2018**, *46* (W1), W257−W263.
(92) Dhokchawle, B. V.; Tauro, S. J.; Bhandari, A. B. Ester Prodrugs of Ketoprofen: Synthesis, Hydrolysis Kinetics and Pharmacological Evaluation. *Drug Res.* **2016**, *66* (01), 46−50.

https://doi.org/10.1021/acsomega.3c05247
ACS Omega 2023, 8, 39490−39510